

國立交通大學

顯示科技研究所

碩士論文

最大輸入編碼色彩重現之
四原色色域最佳化設計



**Optimum Design of Four-primary Color Gamut for
Reproducing Maximum Input Encoded Color**

研究生：陳勇智

指導教授：謝漢萍教授

中華民國 九十六 年 六 月

最大輸入編碼色彩重現之 四原色色域最佳化設計

Optimum design of Four-primary Color Gamut for
Reproducing Maximum Input Encoded Color

研究生：陳勇智
指導教授：謝漢萍

Student : Yong-Jhih Chen
Advisor : Han-Ping D. Shieh

國立交通大學 電機學院

顯示科技研究所

碩士論文

A Thesis

Submitted to Display Institute
College of Electrical Engineering and Computer
Science

National Chiao Tung University
in Partial Fulfillment of the Requirements
for the Degree of Master

in

Display Institute

June 2007

Hsinchu, Taiwan, Republic of China

中華民國 九十六 年 六 月

最大輸入編碼色彩重現之 四原色色域最佳化設計

碩士研究生：陳勇智

指導教授：謝漢萍教授

國立交通大學

顯示科技研究所

摘 要

為擴大顯示器色域以呈現更生動且自然的色彩，近年來已吸引許多顯示器專家及廠商投入多原色技術的發展。相較於傳統顯示器之設計，多原色顯示器保有色域設計的彈性。然而，惟有透過適切的色域轉換之影像編碼，消費者才有機會享受大色域顯示器所呈現的豐富鮮豔色彩。本論文提出重現最大輸入編碼色彩之(四原色)色域最佳化設計的方法。基於最大色域體積重疊的條件，此方法可達到高傳真的色彩重現目的。

為實際比較並驗證基於不同演算法所獲得之最佳化色域，本研究設計一組背光模組（暨驅動電路）作為驗證平台，並採用四原色發光二極體為光源，令該背光模組具備呈現不同色域之彈性。本研究以兩種主要編碼色域—“標準 RGB”及“真實表面色域”作為輸入色域，分別依循兩種常用演算法則—最大白點亮度與最大設計色域體積要求，以及本論文所建議之最大輸入色域體積重疊要求進行計算，並依據所得結果進行交差比對。結果顯示使用本方法可重現最大輸入色域。此外，若應用於最新發展的大色域輸入編碼訊號，將可以使多原色顯示器顯示出更接近人眼視覺系統的色域表現範圍。

Optimum Design of Four-primary Color Gamut for Reproducing Maximum Input Encoded Color

Student: Yong-Jhih Chen

Advisor: Dr. Han-Ping D. Shieh

**Display Institute
National Chiao Tung University**

Abstract

In order to widen the display color gamut for providing more vivid and natural color perception, many of researchers and manufacturers were attracted to invest in the development of multi-primary technology in recent years. Comparing to the conventional displays, multi-primary displays (MPDs) offer the flexibility to adjust and exhibit possible color gamut volume (CGV). However, only through proper encoding gamut conversion, consumers could have the chance to enjoy the vivid color image on the large gamut display. This thesis presents a method to design the optimal (four-primary) color gamut for reproducing maximum number of input encoded color. Based on the maximum color gamut volume intersection requirement, the high-fidelity color reproduction can be achieved.

For actually comparing and evaluating the optimum color gamut based on different algorithms, a backlight module (and the driving circuit) was constructed as a platform for verification. A set of four four-primary LEDs were adopted as the light sources, which offer the flexibility to have the different color gamut on the backlight module. Two major encoding color gamuts, “sRGB” and “real surface color gamut,” are chosen as input gamuts. Calculations are performed under two commonly-adopted criteria, maximum white point luminance and maximum designed CGV, and the proposed one, maximum intersectional CGV, respectively. Result shows the proposed method, compared to others, is demonstrated to reproduce maximum input color gamut. Moreover, if applying the method to the new developed large color gamut input encoding signal, the MPDs will display the color gamut toward the gamut range of human visual system.

誌 謝

首先誠摯的感謝指導老師謝漢萍教授，在這碩士兩年中對於研究態度及英文能力的教導，以及提供豐富的資源與完善研究環境，使我得以在碩士生涯提升了專業及英文的能力，順利完成此論文。此外，也感謝各位口試委員所提供的寶貴意見，使本論文更加的完備。

在此特別感謝鄭裕國學長對於論文的指導，細心的指導方式，嚴謹的研究態度，讓我更能學習成長，受益良多。另外，本論文的完成亦得感謝點晶科技吳華胄先生對於實驗元件的提供，促使實驗平台的完成。

在實驗室的日子裡，感謝有鄭榮安、林芳正、楊柏儒、方仁宇、陳均合、莊喬舜、李企桓等經驗老到、學識豐富的學長姐們提供各方面的指導與協助，同時感謝侑興、坤岳、友群、振宇、韻竹、雅婷等同學們在課業、研究、生活上的幫助與分享，並伴我一起度過兩年碩士班的日子。我也感謝實驗室的學弟妹們與助理小姐，感謝你/妳們的幫忙及讓實驗室充滿歡愉的氣氛。與實驗室成員們歡樂辛酸的每一天，我將銘感在心。

最後，我要呈上我最多的歉意和謝意給予我心愛的女友一貽姍及我最敬愛的家人，他們的體諒和關愛是支持我一路走來最大的支柱，使我能無後顧之憂的研究與學習，並順利完成碩士學業。如今我即將邁入人生的另一個階段，在未來的日子裡我必當竭盡所能來回報你們。在此，我將這份喜悅與每位關心我的人分享。

Table of Contents

Abstract (Chinese)	i
Abstract (English)	ii
Acknowledgment	iii
Table of Contents	iv
Figure Captions	vi
List of Tables	ix
Chapter 1 Introduction	1
1.1 Color gamut of multi-primary display.....	1
1.1.1 Different color gamut	1
1.1.2 Widening color gamut	3
1.1.3 Multi-color-LED backlight in field sequential	4
1.2 Color reproduction.....	7
1.2.1 Gamut mapping	8
1.2.2 Color conversion issues.....	9
1.3 Motivation and objective of this thesis.....	11
1.4 Organization of this thesis	12
Chapter 2 Principle of Color Gamut Design	13
2.1 Colorimetry.....	13
2.1.1 CIEXYZ color space	14
2.1.2 CIELUV color space	15
2.1.3 CIELAB color space.....	17
2.2 Previous work - Wen's method.....	18
2.3 Proposed method	23
2.4 Test input color gamuts.....	27
2.4.1 Standard RGB color space (sRGB)	27
2.4.2 Real-world surface colors gamut.....	29
Chapter 3 Experiment and Simulation	31
3.1 Experiment.....	31

3.1.1 Four-primary-LED backlight platform.....	31
3.1.2 Measurement equipment	34
3.1.3 Measurement data.....	36
3.2 Simulation.....	39
3.2.1 Numerical analysis	39
3.2.2 Gamut visualization.....	39
3.2.3 Q-hull algorithm	40
Chapter 4 Results & Discussion.....	41
4.1 sRGB color gamut as the input.....	41
4.1.1 Maximum white point luminance.....	41
4.1.2 Maximum four-primary CGV	43
4.1.3 Maximum input CGV intersection	44
4.1.4 Summary.....	46
4.2 Real surface color gamut as the input.....	49
4.2.1 Maximum white point luminance.....	49
4.2.2 Maximum four-primary CGV	51
4.2.3 Maximum input CGV intersection.....	52
4.2.4 Summary.....	54
4.3 Discussion.....	57
Chapter 5 Conclusions & Future Work	59
5.1 Conclusions	59
5.2 Future work.....	61
Reference.....	62
Appendix	64

Figure Captions

Fig. 1-1. The CIE xy chromaticity diagram with the color gamuts of NTSC and a.....	2
Fig. 1-2. The displays with different NTSC ratio color gamut.....	3
Fig. 1-3. Timing of the driving scheme of four color LEDs for modulating color gamut.....	5
Fig. 1-4. Illustration of color gamut modulation of four color LEDs.....	5
Fig. 1-5. The white point decided by the relative luminance of four-primary LEDs: (a) a high color temperature setting, (b) a low color temperature setting.....	6
Fig. 1-6. Basic color reproduction process through device-independent color space	7
Fig. 1-7. The gamut transformation of color reproduction process.....	8
Fig. 1-8. The illustration of gamut mapping.....	9
Fig. 2-1. The matching functions fitted to the spectral responses of human eye	15
Fig. 2-2. The volume of visible colors in the CIEXYZ color space, the triangle is on the $X + Y + Z = 1$ plane.....	15
Fig. 2-3. The 1976 $u'v'$ chromaticity diagram and its color difference diagram.....	16
Fig. 2-4. Luminance Y_r , Y_g , and Y_b plotted against Y_y under the white point requirement (S. Wen, Displays, 26, pp. 171-176, 2005)	21
Fig. 2-5. Luminance ratios Y_{rm}/Y_r , Y_{gm}/Y_g , Y_{bm}/Y_b , and Y_{ym}/Y_y plotted against Y_y (S. Wen, Displays, 26, pp. 171-176, 2005)	22
Fig. 2-6. The CGV (ΔE^*ab^3) of four-primary display plotted against Y_y (S. Wen, Displays, 26, pp. 171-176, 2005)	23
Fig. 2-7. The design flow of proposed method.....	26
Fig. 2-8 The Pointer color gamut in CIE xy chromaticity diagram	30
Fig. 3-1. The photo of four-primary-LED backlight platform, which included (a) a optical cavity, (b) a constant-current driving board, and (c) FPGA control signal board	32
Fig. 3-2. The photo of simple optical cavity and the correlative specification of LED	32
Fig. 3-3. The photo of constant-current driving board and its description.....	33
Fig. 3-4. The photo of Conoscope	34

Fig. 3-5. The luminous information path in Conoscope.....	35
Fig. 3-6. The principle diagram of Conoscope.....	36
Fig. 3-7. Four-primary color gamut compared with standard color space in CIE 1976 UCS diagram.....	37
Fig. 3-8. Luminance of each primary plotted against digital count of control circuit.....	37
Fig. 3-9. The plot of different digital count (divided into 8 levels) in the CIE xy chromaticity diagram.....	38
Fig. 3-10. The concept of convex hull in gamut visualization	40
Fig. 3-11. The simple illustration of q-hull algorithm method	40
Fig. 4-1. Plots of luminances Y_r , Y_g , and Y_b as functions of Y_c under the white point requirement.....	42
Fig. 4-2. Plots of luminance ratios Y_{rm}/Y_r , Y_{gm}/Y_g , Y_{bm}/Y_b , and Y_{cm}/Y_c as functions of Y_c under the white point requirement.....	43
Fig. 4-3. The available LED efficiency plotted against Y_c under the sRGB gamut input.....	43
Fig. 4-4. The four-primary CGV plotted against Y_c under the sRGB gamut input.....	44
Fig. 4-5. Plot of intersectional CGV as a function of the shifted Y_c value under sRGB gamut input.....	45
Fig. 4-6. 3D visualization of four-primary gamut in CIELAB color space with different angle of (a) top and (b) side view	45
Fig. 4-7. 3D visualization of sRGB color gamut in CIELAB color space with different angle of (a) top and (b) side view	46
Fig. 4-8. 3D CGV Intersection of four-primary gamut and sRGB gamut.....	46
Fig. 4-9. Efficiency, four-primary CGV, and the intersectional CGV plotted against Y_c for comparison with sRGB gamut input	47
Fig. 4-10. Plots of luminances Y_r , Y_g , and Y_b as functions of Y_c under the white point requirement.....	50
Fig. 4-11. Plots of luminance ratios Y_{rm}/Y_r , Y_{gm}/Y_g , Y_{bm}/Y_b , and Y_{cm}/Y_c as functions of Y_c under the white point requirement.....	51
Fig. 4-12. The available LED efficiency plotted against Y_c under real surface gamut input..	51

Fig. 4-13. The four-primary CGV plotted against Y_c under the real surface gamut input 52

Fig. 4-14. Plot of intersectional CGV as a function of the shifted Y_c value under real surface gamut input..... 53

Fig. 4-15. 3D visualization of four-primary gamut in CIELAB color space with different angle of (a) top and (b) side view..... 53

Fig. 4-16. 3D visualization of real surface color gamut in CIELAB color space with different angle of (a) top and (b) side view 54

Fig. 4-17. 3D CGV Intersection of four-primary gamut and real surface color gamut..... 54

Fig. 4-18. Efficiency, four-primary CGV, and the intersectional CGV plotted against Y_c for comparison with real surface gamut input..... 55

Fig. 5-1. The algorithm of two type gamut mappings of the large gamut display 61



List of Tables

Table 2-1 Parameters of sRGB chromaticities.....	28
Table 2-2 Parameters of sRGB viewing environment.....	29
Table 3-1 LED specifications and measurement data	36
Table 4-1 The relative luminance setting of each criterion with sRGB gamut input	47
Table 4-2 The compared result of each criterion.....	48
Table 4-3 The color difference with the reference white D65 in CIE 1976 UCS diagram of each criterion.....	48
Table 4-4 The relative luminance setting of each criterion with real surface gamut input	54
Table 4-5 The compared result of each criterion.....	56
Table 4-6 The color difference with the reference white C in CIE 1976 UCS diagram of each criterion.....	56
Table 4-7 The simplified comparison of each criterion.....	57



Chapter 1

Introduction

Color gamut [1], the range of color which can be reproduced by a device, is one of the general index to judge the color performance of a display. For widening the color gamut, several multi-primary displays (MPDs) [2], [3] were proposed to achieve vivid and natural color perception. However, the additional primaries will bring the color conversion issue due to the offered flexibility in color reproduction process [4]. In this chapter, the key issues of color gamut design in MPDs and the objective of this thesis will be discussed.

1.1 Color gamut of multi-primary display



1.1.1 Different color gamut

Color gamut of a device or a system is often quantified by comparison with National Television System Committee (NTSC) [5] standard in some engineering applications. The NTSC is the analog color television (TV) standard in the United States and defines the color and video information. The percentage of NTSC in the chromatic diagram is the reference index, which implies the approximate ratio of total color that can be theoretically displayed in a color TV system. As shown in Fig. 1-1, the color gamut is presented in the CIE 1931 xy chromaticity diagram. The horseshoe-shaped border represents the visual spectrum boundary of human eye. The gamut of NTSC and a typical liquid crystal display (LCD) [6] are represented by the solid- and dashed- line triangles, respectively. As shown in the diagram, the color gamut of typical LCD is only 70% of NTSC and also far less than the gamut that human

eye can see. Actually, the color gamut showed and compared in 2D chromaticity diagram just for convenience. The “real color gamut” is operated and visualized in the three dimensional color spaces, which will be described in next chapter.

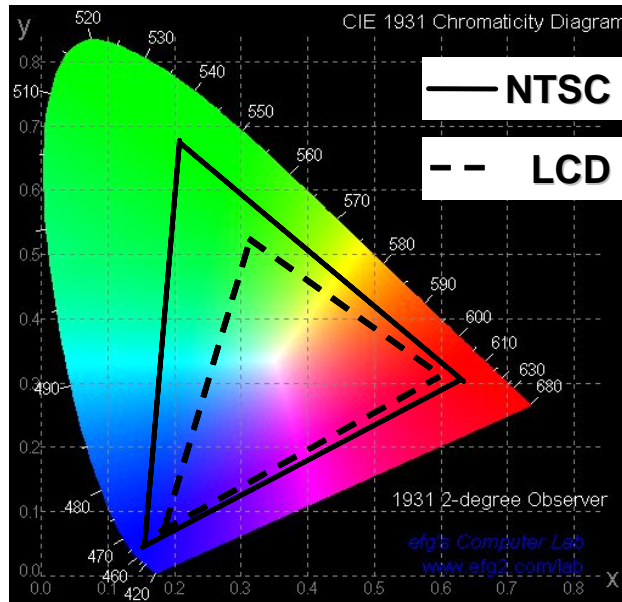


Fig. 1-1. The CIE xy chromaticity diagram with the color gamuts of NTSC and a typical LCD

Since the performance of color is now receiving considerable attention in display technology, larger color gamut display for presenting more color and higher color saturation image is increasing demand from display manufacturers. The performances of two commercial LCDs with different color gamut are shown in Fig. 1-2. The right LCD, which has 90% of NTSC is much larger than the left one, which only has 72% of NTSC. Obviously, the right one which has the larger gamut performs the more vivid and natural color perception than the left one.

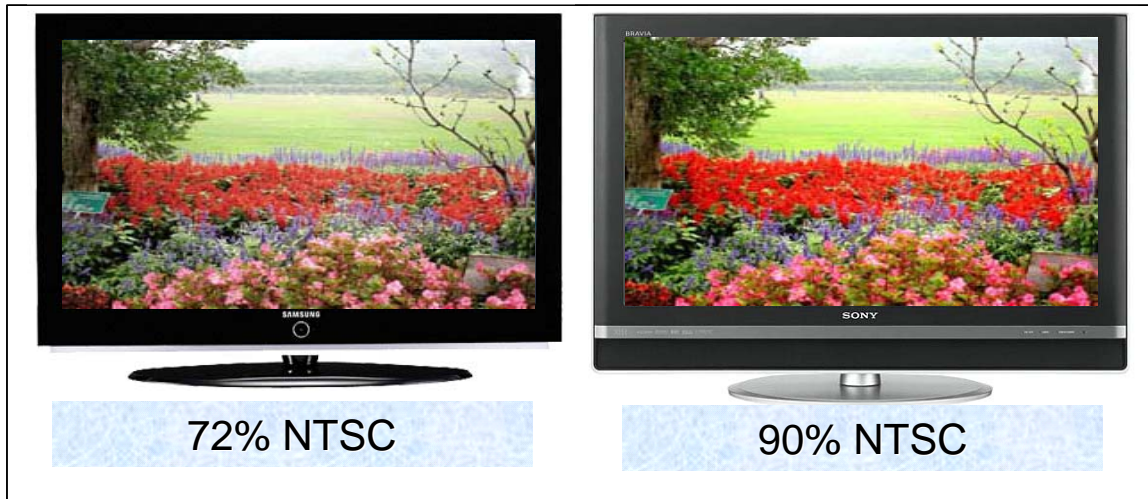


Fig. 1-2. The displays with different NTSC ratio color gamut

1.1.2 Widening of color gamut

Currently, there are two major methods proposed for widening the color gamut of displays. The first use the saturated primaries [7], and the second use the multi-primaries [8].

For example, the color gamut of recent most important information display device, LCD, is determined by the combination of the spectral characteristics of backlight source and the spectral transmission factors of color filters. Since the conventional light source, cold cathode fluorescent lamp (CCFL), has the wider band spectrum, some lights leak to the not intended wavelength of color filters result in a poor color separation. For providing the saturated primaries with narrow spectrum, some researchers replaced CCFL with the light-emitting diode (LED) [7], thus making it easier to separate colors by the color filters.

Besides the above mentioned proposal, the most efficient way to enlarge the color gamut of display significantly was to increase the number of primaries. Therefore, some researches proposed and demonstrated the MPDs either of the sequential or spatial type to increase the color gamut [9], [10].

1.1.3 Multi-color-LED backlight in field sequential

As previously noted, multi-primary display (MPD) is the proper method to widen the color gamut. A four-primary-LED backlight in the field-sequential full-color (FS-FC) LCDs [11] was proposed, due to its high luminous efficiency and large color gamut. Furthermore, the extra advantages to modulate the color gamut and color temperature efficiently were brought simultaneously. Thus, this thesis based on this structure examines the proposed method in the following chapter.

Modulation of the color gamut

Since the FS-FC LCD replaces the color filters with the color sequential LED backlight, the effective primaries or color gamut are decided by the sequential LED signals and transmitted characteristic of the liquid crystal. For example, the timing of driving scheme of the four color LEDs is schematically represented in Fig. 1-3. As shown in Fig. 1-3(a), when sequentially turn on the four LED backlights R, G1, B, and G2, the quadrangle color gamut will be much larger than the NTSC color gamut in the chromaticity diagram, as shown in Fig. 1-4. Moreover, if G1 and G2 are operated simultaneously, as shown in Fig. 1-3(b), the coordinate of G' (refer to Fig. 1-4) is the result from the combination of G1 and G2 by properly tuning the relative luminance. Then, the effective dynamic three primary color gamut RG'B can be adjusted by preference design.

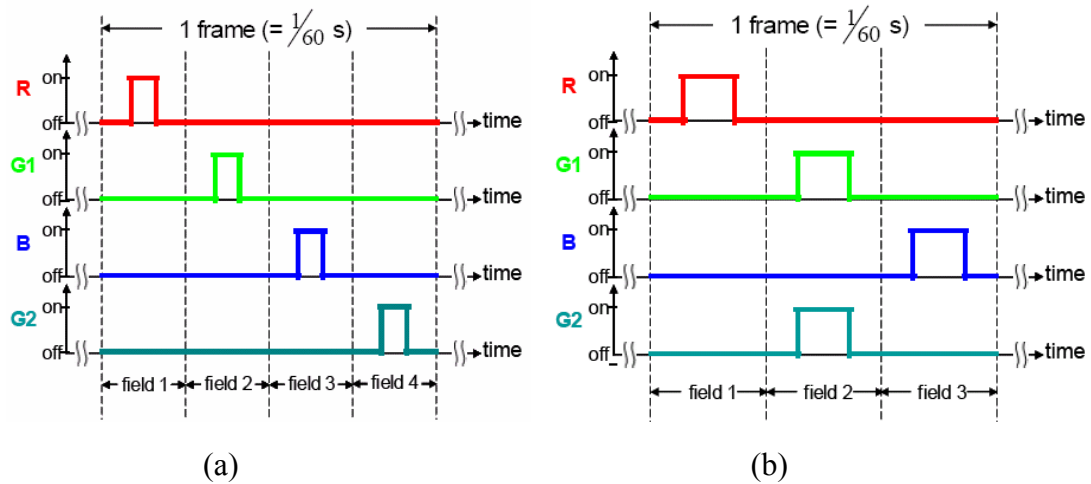


Fig. 1-3. Timing of the driving scheme of four color LEDs for modulating color gamut : (a) Sequential turn on RG1BG2 LEDs, (b) G1 and G2 are operated in the same field

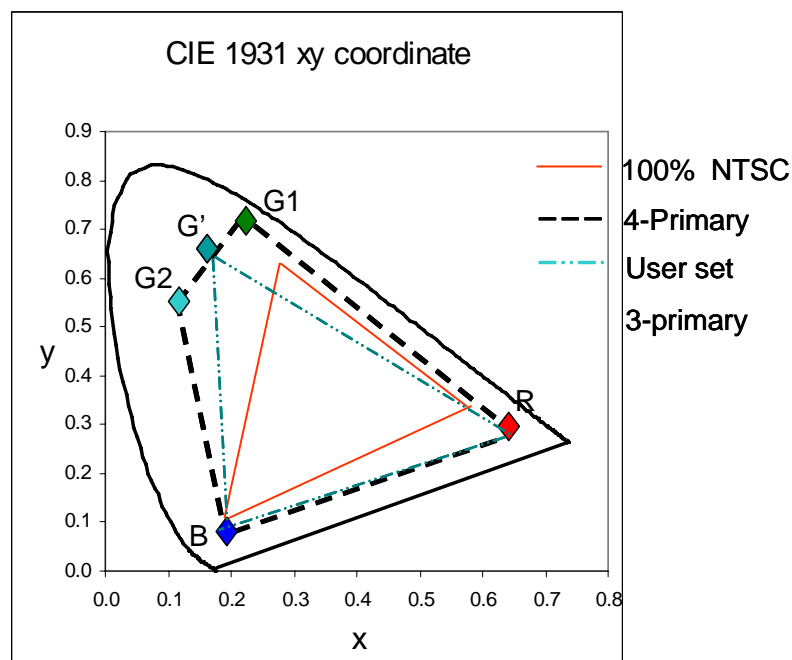
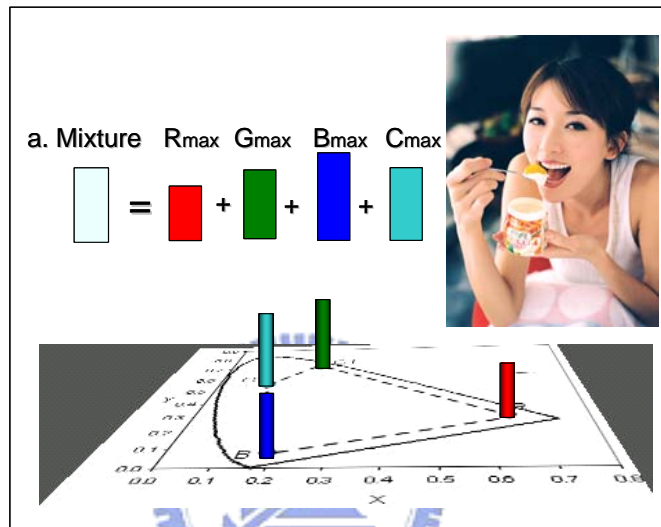


Fig. 1-4. Illustration of color gamut modulation of four color LEDs

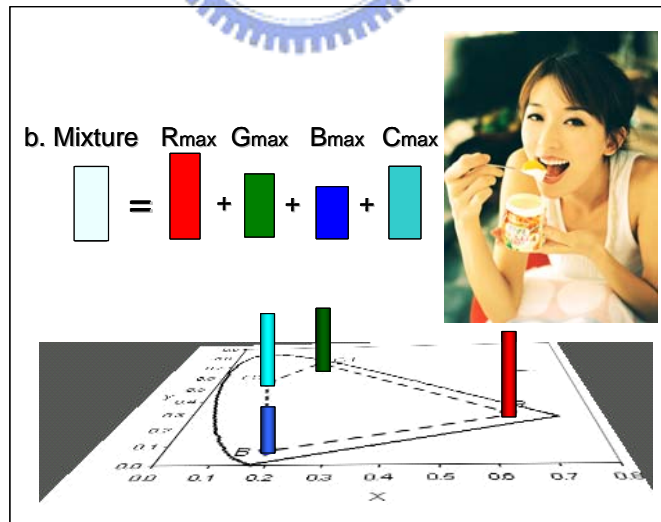
Modulation of the color temperature

Color temperature that dominantly affects the color performance is the characteristic of the white point of a display, and the white point is decided by the relative luminance of each primary. Due to the very nature of field sequential method and the current-controlled LEDs, the desired color temperature can be obtained by applying well-calculated timing and driving

current to each LED of the backlight system. After the calculation, operating currents of each LED are acquired to drive the LEDs to achieve the target color temperature. As shown in Fig. 1-5, Fig. 1-5(a) is the high color temperature setting and Fig. 1-5(b) is the low color temperature setting, each having different relative ratio of primaries that performs different perceptions. Since the LEDs are separately controlled, it is easy to modulate the color temperature of LCDs by tuning the proportionality of luminance between the primary colors.



(a)



(b)

Fig. 1-5. The white point decided by the relative luminance of four-primary LEDs: (a) a high color temperature setting, (b) a low color temperature setting

1.2 Color reproduction

Many types of electronic imaging devices, including color cathode ray tube (CRT) devices, ink jet printers, LCDs, etc. utilize the device-dependent color spaces for color specification. However, device-dependent color spaces do not relate to an objective definition of color or human color perception. Therefore, the device-independent color spaces [12] developed by International Commission on Illumination (CIE) give a quantitative measure for all colors that is not dependent on the imaging device. As a result, the production of color consistency between various devices, i.e., the concept of device-independent color reproduction, as shown in Fig. 1-6, has been received widespread attention.

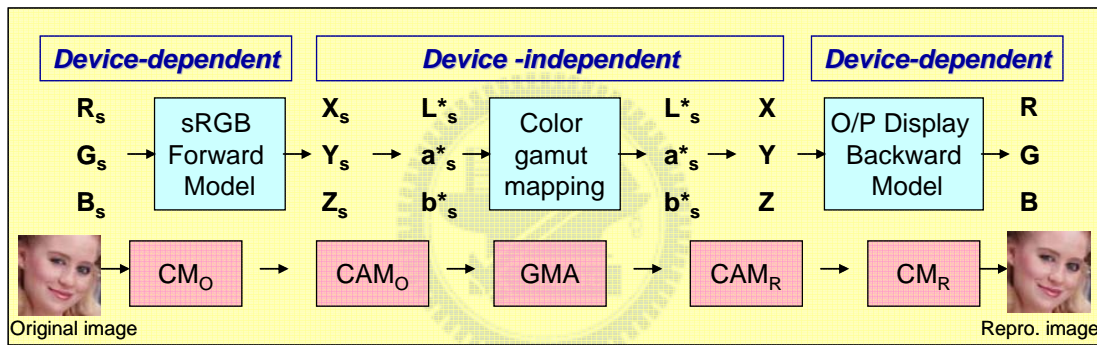


Fig. 1-6. Basic color reproduction process through device-independent color space

The six types of color reproduction were defined by Hunt [13] as follows: spectral color reproduction, colorimetric color reproduction, exact color reproduction, equivalent color reproduction, corresponding color reproduction, and preferred color reproduction. Each of these types of color reproduction is separated according to purpose. Nowadays, the research related to reproducing images on MPD was classified into two main areas. The first one was based on multi-spectral information [14], such as the spectral reflectance of an object estimated by a multi-spectral camera or some measured spectrum data. This type of reproduction tends to reproduce the original color, i.e., natural color reproduction, which can reproduce more realistic image, but can not be directly applied to current High-definition

television (HDTV) system. The other one was based on the colorimetric information [15], such as standard RGB (sRGB) and CIEXYZ, for applying the current color management system. This type of reproduction also can reproduce the original color and tend to reproduce the preference color, i.e., preference color reproduction [16], which can produce the memory color of people preferred but need some psychophysical experiment to be evaluated. In this thesis, the measured colorimetric data was applied for the original color reproduction.

1.2.1 Gamut mapping

The color reproduction from the input color gamut to multi-primary color gamut needs a transformation, called gamut mapping, as shown in Fig. 1-7. The gamut mapping is a technique to transform out-of-gamut colors into within-gamut, and thereby solve the gamut-mismatch problem. Since the destination gamut of MPD is larger than the recent input color gamut, the mapping can be the original color mapping or preference color mapping. Furthermore, the gamut mapping is implemented in the device-independent color space, which is represented in three dimensions (3D), as shown in Fig. 1-8. Over the years, some strategies [17] has been using to solve the variant gamut mapping problem.

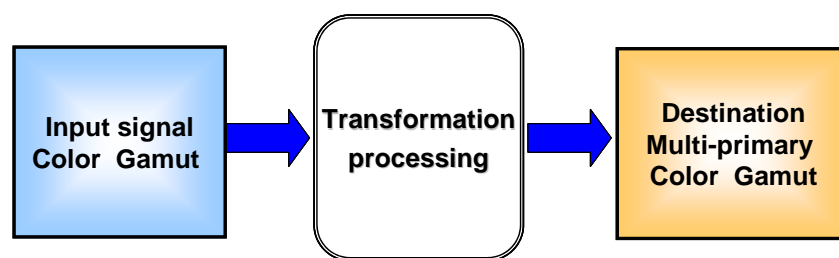


Fig. 1-7. The gamut transformation of color reproduction process

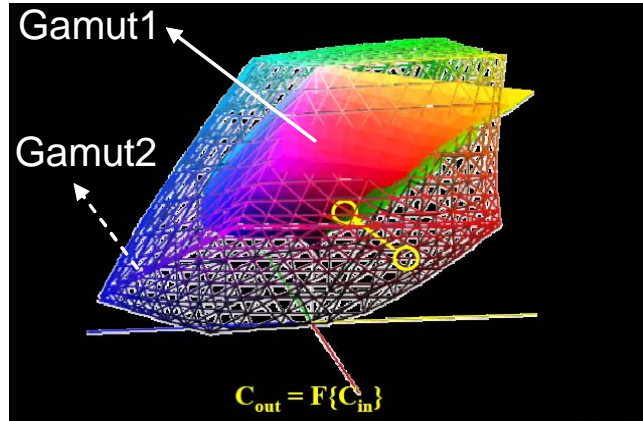


Fig. 1-8. The illustration of gamut mapping

1.2.2 Color conversion issues

As previously noted, the device-independent color space provided by CIE is utilized for the color reproduction, and the device-independent color reproduction requires a color conversion between device color and device-independent color to achieve color consistency. Any color in a three primary system can only be expressed as a single combination of coordinates. For example, the relative primary luminances of a conventional three-primary display are uniquely determined by its white point. Refer to Fig. 1-6, in that case, the linearity and additivity of colorimetric characteristics of a display system are ensured; the forward model is shown as follows:

$$\begin{bmatrix} X_w \\ Y_w \\ Z_w \end{bmatrix} = \begin{bmatrix} X_{R_max} & X_{G_max} & X_{B_max} \\ Y_{R_max} & Y_{G_max} & Y_{B_max} \\ Z_{R_max} & Z_{G_max} & Z_{B_max} \end{bmatrix} \begin{bmatrix} R \\ G \\ B \end{bmatrix}, \quad \begin{bmatrix} R \\ G \\ B \end{bmatrix} = \begin{bmatrix} TRC(d_R) \\ TRC(d_G) \\ TRC(d_B) \end{bmatrix} \quad (1-1)$$

where R/G/B are the three primaries, Xi/Yi/Zi are the CIE XYZ tristimulus, di is the display signal, and TRC is a tone reproduction curve. Note: [i can be the three primaries (R, G, and B) and the white point (w)]. Then, a backward model defined as the inversion of a forward mode, is shown as follows:

$$\begin{bmatrix} R \\ G \\ B \end{bmatrix} = \begin{bmatrix} X_{R_max} & X_{G_max} & X_{B_max} \\ Y_{R_max} & Y_{G_max} & Y_{B_max} \\ Z_{R_max} & Z_{G_max} & Z_{B_max} \end{bmatrix}^{-1} \begin{bmatrix} X_w \\ Y_w \\ Z_w \end{bmatrix}, \quad \begin{bmatrix} d_R \\ d_G \\ d_B \end{bmatrix} = \begin{bmatrix} TRC^{-1}(R) \\ TRC^{-1}(G) \\ TRC^{-1}(B) \end{bmatrix} \quad (1-2)$$

regarding the color management system, to solve the three linear equations in three unknowns, the signal d_i can be calculated by the white point of display.

When the color conversion method applies on the MPD, such as the four-primary backlight, the forward model can be shown as follows:

$$\begin{bmatrix} X \\ Y \\ Z \end{bmatrix} = \begin{bmatrix} X_{R_max} & X_{G_max} & X_{B_max} & X_{C_max} \\ Y_{R_max} & Y_{G_max} & Y_{B_max} & Y_{C_max} \\ Z_{R_max} & Z_{G_max} & Z_{B_max} & Z_{C_max} \end{bmatrix} \begin{bmatrix} R \\ G \\ B \\ C \end{bmatrix}, \quad \begin{bmatrix} R \\ G \\ B \\ C \end{bmatrix} = \begin{bmatrix} TRC(d_R) \\ TRC(d_G) \\ TRC(d_B) \\ TRC(d_C) \end{bmatrix} \quad (1-3)$$

where C, cyan, is the additive primary of the backlight system. In this model, the white point can be achieved by the setting of four-primary signals. However, the backward model of four-primary is shown as follows:

$$\begin{bmatrix} R \\ G \\ B \\ C \end{bmatrix} = \begin{bmatrix} X_{R_max} & X_{G_max} & X_{B_max} & X_{C_max} \\ Y_{R_max} & Y_{G_max} & Y_{B_max} & Y_{C_max} \\ Z_{R_max} & Z_{G_max} & Z_{B_max} & Z_{C_max} \end{bmatrix}^{-1} \begin{bmatrix} X \\ Y \\ Z \end{bmatrix}, \quad \begin{bmatrix} d_R \\ d_G \\ d_B \\ d_C \end{bmatrix} = \begin{bmatrix} TRC^{-1}(R) \\ TRC^{-1}(G) \\ TRC^{-1}(B) \\ TRC^{-1}(C) \end{bmatrix} \quad (1-4)$$

There is an issue in Eq. (1-4), i.e., the three linear equations in four unknowns result in numerous combinations and permutations of coordinates. In this case, Eq. (1-4) remains one degree of freedom for choosing the relative primary luminances at the given white point. Finding a constraint can determine the unique multi-primary color decomposition.

1.3 Motivation and objective of this thesis

The conventional display devices based on three primary colors cannot cover the entire color gamut perceived by human visual system. In order to extend more vivid and natural color perception, several methods, such as using saturated primaries and/or multiple primaries, had been developed for increasing the color gamut of LCDs. Furthermore, a proposed four-primary-LED backlight in the FS-FC LCDs also has advantage to modulate the color gamut and color temperature efficiently.

Although the color gamut can be widened by using multi-color LEDs, there are some color conversion issues on designing the color gamut volume (CGV) in MPDs. Comparing to the conventional displays, MPDs offer the flexibility to adjust and exhibit possible CGV. Wen [18] proposed the maximum white point luminance and the maximum CGV requirements for a four-primary display. However, the volume and shape of the device gamut are two of the key factors that determine color reproducibility. When the input encoded color gamut is considered, the maximum CGV may be not suitable for the input color reproduction.

In this thesis, the author refers to the methods proposed by Wen and proposes a method for designing a four-primary CGV with maximum input encoded CGV intersection that providing maximum input color reproduction. The high-fidelity color reproduction is expected to be achieved by this method.

1.4 Organization of this thesis

The thesis is organized as followings: The theories of colorimetry and design of color gamut are presented in **Chapter 2**. Basic colorimetry concepts for presenting CGV are described in this chapter. Additionally, this chapter also represents the criteria of four-primary color gamut design. In **Chapter 3**, the experiment of four-primary LED backlight platform is introduced in detail. Furthermore, the major instruments used to measure the color data and the simulate method are also described. After that, the experimental results, including the two test input color spaces and the discussions of comparison, are presented in **Chapter 4**. Finally, the conclusions and future work are given in **Chapter 5**.



Chapter 2

Principle of Color Gamut Design

The most primitive theory of colorimetric with respect to the CGV representation will be reviewed. Besides, the previous method of four-primary color gamut design will be interpreted briefly as well. Finally, the proposed method and the two test input color gamuts for evaluating the gamut designing methods will be introduced separately.

2.1 Colorimetry

Colorimetry is the science relating color comparison and matching. To describe colors in numbers or to provide the physical or psychophysical color match using a variety of measurement instruments are all about colorimetry. The matching in color of two light stimuli of different spectral power distributions under a given condition of observation can be predicted by using basic colorimetry. Over the years, The CIE has defined a set of standard observers and standard conditions for performing color matching experiments. The color matching functions defined by color matching experiment is the basis of colorimetry. Using this color matching functions, the various color spaces have been developed for denoting colors numerically [19], [20], [21].

A color space is a mathematical multidimensional coordinate system where each dimension corresponds to a color component. Mathematically, a color is a vector in a color space, and the color gamut of a device is the subset of available colors in the color space. A device-dependent color space is one in which the same combination of color values on two different devices does not produce the same visual color. On the other hand, in a

device-independent color space, the same set of tri-stimulus values produces the same visual color on two different devices at the same viewing condition. As mentioned earlier, the color reproduction prefers to perform in the device-independent color spaces. The various device-independent color spaces are introduced in the following section.

2.1.1 CIEXYZ color space

In 1931, the CIE agreed on a device-independent standard color space called CIEXYZ, which was created in the need for describing colors in the mathematical equivalent way. The color was measured with tristimulus filters corresponding to the sensitivities of the receptors in the standard observer. The result was the functions of matching curves fitted to the detected wavelengths, as shown in Fig. 2-1. Then, the integrations of matching function multiplying the object and illumination reflectance were computed as tristimulus values: X, Y and Z. However, the tristimulus values were virtual tristimulus, and describing color in the three dimensions was not convenient. A derived color space specified by x, y, and Y was known as the CIE xyY color space. As shown in Fig. 2-2, the x and y is the coordinate of specific color on $X + Y + Z = 1$ plane by using the following equations: [22]

$$\begin{aligned}x &= \frac{X}{X + Y + Z} \\y &= \frac{Y}{X + Y + Z} \\z &= \frac{Z}{X + Y + Z}\end{aligned} \tag{2-1}$$

The third coordinate, z, can be omitted by providing Y parameter which is a measure of the luminance of a color. As a result, the chromaticity description of any color by using just two coordinates on the projecting locus of that plane, the CIE xy chromaticity diagram, is widely used in practice.

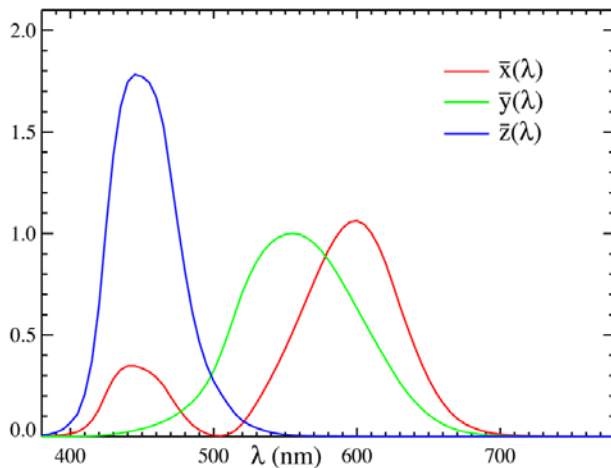


Fig. 2-1. The matching functions fitted to the spectral responses of human eye

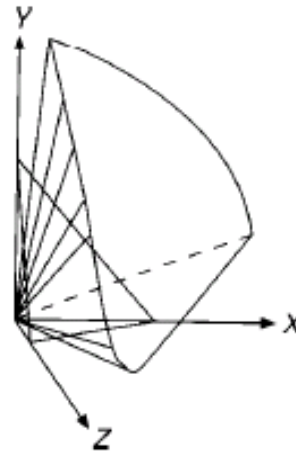


Fig. 2-2. The volume of visible colors in the CIEXYZ color space, the triangle is on the $X + Y + Z = 1$ plane

The CIEXYZ system is widely used to specify colors; however, the chromaticity diagram is highly non-uniform. In the CIEXYZ system, a vector of unit magnitude representing the difference between two chromaticities is not uniformly visible [23]. The CIEXYZ is not suitable for judging the color difference. So the CIELUV and CIELAB color spaces were developed for solving this problem.

2.1.2 CIELUV color space

The CIE 1960 u', v' (UCS) diagram was the first determined by the linear transformation of Yxy , in an attempt to produce a chromaticity diagrams, in which a vector of unit magnitude difference is equally visible at all colors as shown in Fig 2-3. Y is unchanged from XYZ or Yxy . The non-uniformity is reduced considerably, but the uniform brightness scale is not included.

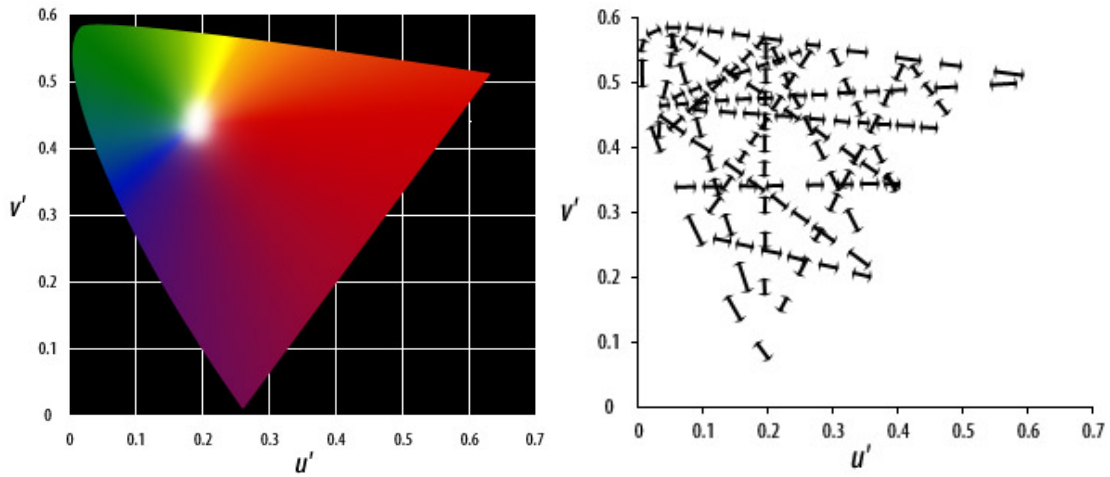


Fig. 2-3. The 1976 $u'v'$ chromaticity diagram and its color difference diagram

Base on the CIE 1960 $u'v'$ diagram, the CIE developed the CIE 1976 UCS diagram transformed from Yxy and defined the CIE 1976 $L^*u^*v^*$ (CIELUV) space involves the uniform lightness scale. The transform was given by

$$L^* = 116f\left(\frac{Y}{Y_n}\right) - 16 \quad (2-2)$$

$$\begin{cases} u^* = 13L^*(u' - u'_n) \\ v^* = 13L^*(v' - v'_n) \end{cases} \quad (2-3)$$

where

$$\begin{cases} f(k) = \sqrt[3]{k} & \text{if } k > 0.08856 \\ f(k) = 7.87k + \frac{16}{116} & \text{if } k \leq 0.08856 \end{cases} \quad (2-4)$$

$$\begin{cases} u' = \frac{4X}{X + 15Y + 3Z} \\ v' = \frac{9Y}{X + 15Y + 3Z} \end{cases} \quad (2-5)$$

$$\begin{cases} u_n' = \frac{4X_n}{X_n + 15Y_n + 3Z_n} \\ v_n' = \frac{9Y_n}{X_n + 15Y_n + 3Z_n} \end{cases} \quad (2-6)$$

where X_n , Y_n , and Z_n are the tristimulus of the reference white. The u' and v' are the chromaticity coordinates of stimulus, the u'_n and v'_n are the chromaticity coordinates of reference white.

2.1.3 CIELAB color space

The CIE 1976 $L^*a^*b^*$ color space, abbreviated CIELAB, is another uniform color space that transformed from CIEXYZ color space and related to Munsell color system. Three color values L^* (lightness), a^* (red-green axis), b^* (yellow-blue axis) calculated from the CIE tristimulus values. As shown in the follows:

$$L^* = 116f\left(\frac{Y}{Y_n}\right) - 16 \quad (2-7)$$

$$\begin{cases} a^* = 500\left[f\left(\frac{X}{X_n}\right) - f\left(\frac{Y}{Y_n}\right)\right] \\ b^* = 200\left[f\left(\frac{Y}{Y_n}\right) - f\left(\frac{Z}{Z_n}\right)\right] \end{cases} \quad \text{for} \quad (2-8)$$

$$\begin{cases} f(k) = \sqrt[3]{k} & \text{if } k > 0.08856 \\ f(k) = 7.87k + \frac{16}{116} & \text{if } k \leq 0.08856 \end{cases}$$

where X_n , Y_n and Z_n are also the tristimulus values for the reference white, and L^* ranges from 0 to 100, where 0 is perfect black, and 100 is the reference white.

The counterclockwise angle between the positive a^* axis and the vector from the origin to the color is referred to as hue angle. Hue angle h_{ab} and chroma C^*_{ab} are defined as follows:

$$h_{ab} = \arctan\left(\frac{b^*}{a^*}\right)$$

$$C_{ab}^* = \sqrt{(a^*)^2 + (b^*)^2} \quad (2-9)$$

The CIELAB color difference ΔE_{ab}^* between two points is calculated as the Euclidean distance:

$$\Delta E_{ab}^* = \sqrt{(\Delta L^*)^2 + (\Delta a^*)^2 + (\Delta b^*)^2} \quad (2-10)$$

Since the CIELAB is the uniform device-independent color space, the color gamut and the gamut mapping process usually represent in the CIELAB space.

2.2 Previous work - Wen's method

Although many of multi-primary displays were proposed for wider gamut representation, there were only few papers discussed its color gamut design and method. As previous noted, the shape and volume of device gamut will affect the color reproducibility. In addition, the MPDs offer the flexibility to adjust and exhibit possible CGV, and need the constraint to overcome the color conversion. So a previous method for design the relative luminance of four-primary display to decide its color gamut was proposed by Wen [24].

Wen had proposed two criteria to solve this problem, one was the Maximum White Point Luminance (display luminance) requirement, and the other was Maximum CGV requirement. Both of them were base on the basic white point requirement. A four-primary display was taken an example for showing the methods; it is the same condition with this thesis.

For the maximum white point luminance requirement, first of all, the gamut setting was basically meeting the white point of the choosing system. For conventional three primary displays, the relative luminances of primaries were uniquely determined by the white point of display [25]. Utilizing the Grassman's law, the white point tristimulus are the linear

combination of three primaries; the forward model refers to Eq. (1- 1) can be represented as follows:

$$\begin{bmatrix} X_w \\ Y_w \\ Z_w \end{bmatrix} = \begin{bmatrix} X_R & X_G & X_B \\ Y_R & Y_G & Y_B \\ Z_R & Z_G & Z_B \end{bmatrix} \begin{bmatrix} R \\ G \\ B \end{bmatrix} \quad (2-11)$$

and refer to Eq. (1- 2) the relative luminance can be calculated by the backward model:

$$\begin{bmatrix} R \\ G \\ B \end{bmatrix} = \begin{bmatrix} \frac{x_r}{y_r} & \frac{x_g}{y_g} & \frac{x_b}{y_b} \\ 1 & 1 & 1 \\ \frac{z_r}{y_r} & \frac{z_g}{y_g} & \frac{z_b}{y_b} \end{bmatrix}^{-1} \begin{bmatrix} \frac{x_w}{y_w} \\ 1 \\ \frac{z_w}{y_w} \end{bmatrix} \quad (2-12)$$

where (x_r, y_r) , (x_g, y_g) , and (x_b, y_b) are the color coordinates of red, green, and blue primaries; and (x_w, y_w) is the color coordinate of white point.

For the four-primary LED display which Wen used, the additive fourth color is yellowish-green, which is denoted in G_y , enlarging the gamut about 130% NTSC in 1931 CIE xy chromaticity diagram and 137% NTSC in CIE 1976 uniform chromaticity scale (UCS) diagram. To achieve the white point, the forward model refers to Eq. (1- 3) as shown following:

$$\begin{bmatrix} X_w \\ Y_w \\ Z_w \end{bmatrix} = \begin{bmatrix} X_R & X_G & X_B & X_y \\ Y_R & Y_G & Y_B & Y_y \\ Z_R & Z_G & Z_B & Z_y \end{bmatrix} \begin{bmatrix} R \\ G \\ B \\ G_y \end{bmatrix} \quad (2-13)$$

As previous noted, the backward model of four-primary in Eq. (2-13) can not be calculated. For solving the linear equations, there must add some constraint to reduce the

column of matrix. As the definition of white point is the equal energy of each primary, it can be achieved by the $R=B=G=Y_y$ setting, where the normalized white point luminance is the sum of four primaries, as shown following:

$$Y_r + Y_g + Y_b + Y_y = Y_w = 1 \quad (2-14)$$

where $0 \leq Y_r, Y_g, Y_b, Y_y \leq 1$, and Y_r, Y_g, Y_b, Y_y are the relative luminances of each primary. Furthermore, the simple tristimulus derived formula as shown following.

$$Z = \frac{(1-x-y)}{y} Y, \quad X = \frac{x}{y} Y \quad (2-15)$$

As Eqs. (2-14) and (2-15) were applied for Eq. (2-13), the basic color conversion can get the backward model of relative luminance of four primaries:

$$\begin{bmatrix} Y_r \\ Y_g \\ Y_b \end{bmatrix} = \begin{bmatrix} \frac{x_r}{y_r} & \frac{x_g}{y_g} & \frac{x_b}{y_b} \\ 1 & 1 & 1 \\ \frac{z_r}{y_r} & \frac{z_g}{y_g} & \frac{z_b}{y_b} \end{bmatrix}^{-1} \begin{bmatrix} \frac{x_w - x_y}{y_w - y_y} Y_y \\ 1 - Y_y \\ \frac{z_w - z_y}{y_w - y_y} Y_y \end{bmatrix} \quad (2-16)$$

From Eq. (2-16), $Y_r, Y_g,$ and Y_b are dependent on linear function of Y_y . The plotted curve of $Y_r, Y_g,$ and Y_b against Y_y by increasing Y_y , is shown in Fig. 2-4. The figure depicts that each combination of vertical line agrees with the white point setting, and the combination reduce to three primaries, when Y_y at 0 and 0.715.

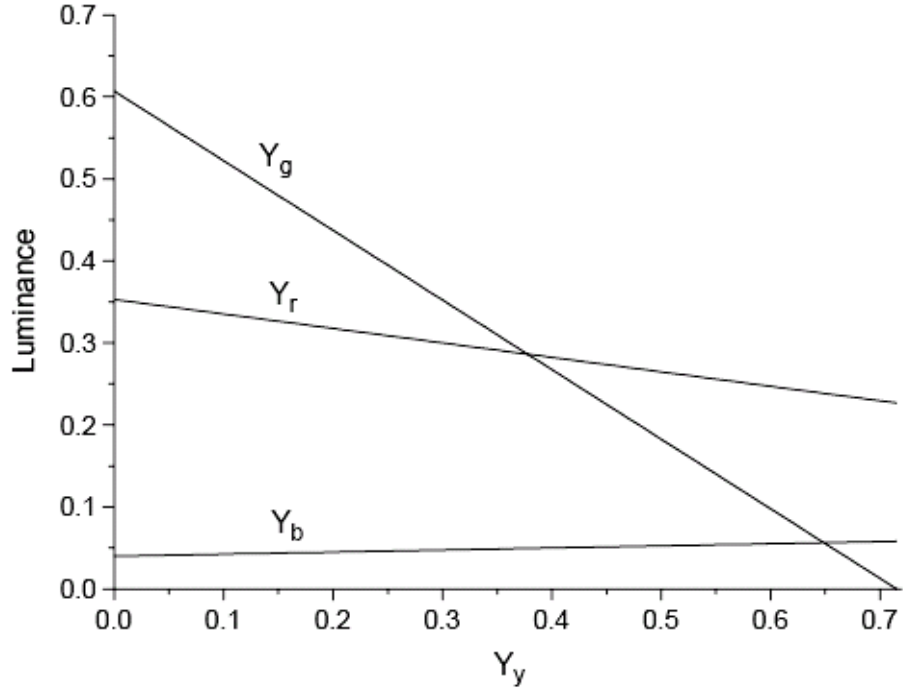
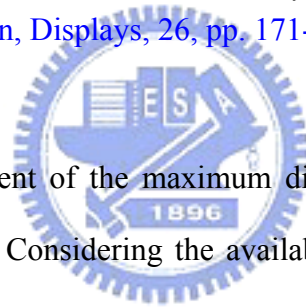


Fig. 2-4. Luminance Y_r , Y_g , and Y_b plotted against Y_y under the white point requirement (S. Wen, *Displays*, 26, pp. 171-176, 2005)



In addition, the requirement of the maximum display luminance is taken for a set of available primary luminances. Considering the available luminance of each LED Y_{rm} , Y_{gm} , Y_{bm} , and Y_{ym} , the white point is satisfied when the

$$\frac{a_r Y_{rm}}{Y_r} = \frac{a_g Y_{gm}}{Y_g} = \frac{a_b Y_{bm}}{Y_b} = \frac{a_y Y_{ym}}{Y_y} = \eta \quad (2-17)$$

$$\text{where } 0 \leq a_r, a_g, a_b, a_y \leq 1, \quad Y_{im} = \frac{\text{Max luminance } i}{\sum_{r,g,b,y} \text{Max luminance } k} \quad i = r, g, b, y \quad (2-18)$$

In Eq. (2-17), a_r , a_g , a_b , and a_y are the turning factor of red, green, blue, and yellowish-green primaries. To meet the maximum efficiency, the desired η is preferred as large as it can be. Therefore, the designed maximum efficiency of four LEDs η_{\max} is defined as

$$\eta_{\max}(Y_y) = \text{Min} \left\{ \frac{Y_{rm}}{Y_r} = \frac{Y_{gm}}{Y_g} = \frac{Y_{bm}}{Y_b} = \frac{Y_{ym}}{Y_y} \right\} \quad (2-19)$$

where $\text{Min} \{ \}$ is the minimum function. By using Eqs. (2-16) and (2-19), the changed relative luminance of yellowish-green Y_y can get the curve plotted in Fig. 2-5 from which the maximum efficiency η_{\max} of 0.908 at $Y_y=0.44$ can be derived. Thus, the initial four-primary color gamut with maximum white point luminance requirement is defined, when $Y_y=0.44$, $Y_r=0.3$, $Y_g=0.24$, and $Y_b=0.05$, respectively.

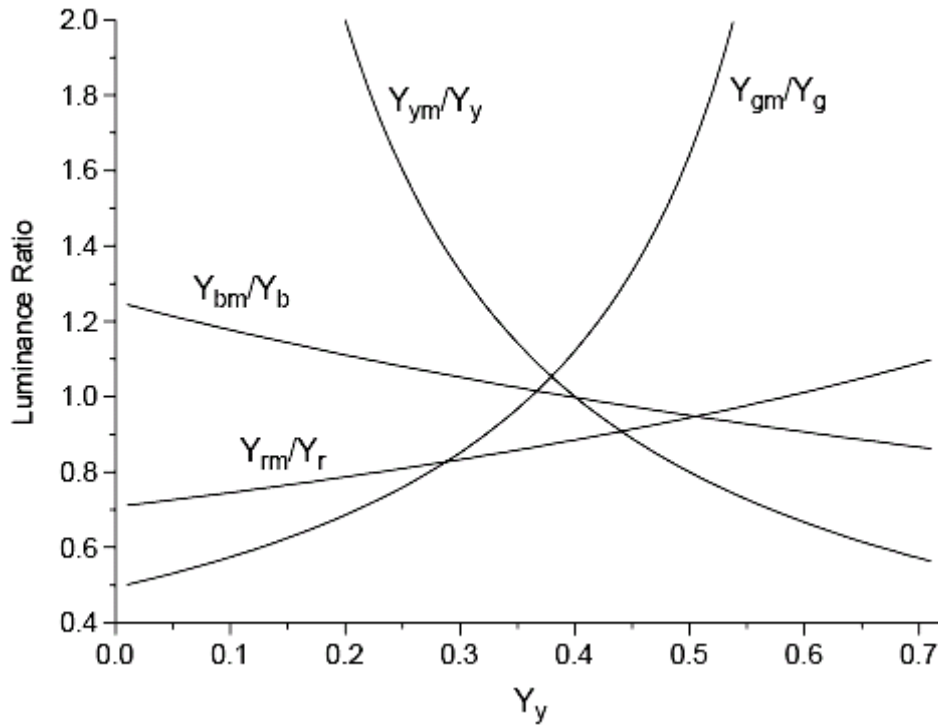


Fig. 2-5. Luminance ratios Y_{rm}/Y_r , Y_{gm}/Y_g , Y_{bm}/Y_b , and Y_{ym}/Y_y plotted against Y_y (S. Wen, Displays, 26, pp. 171-176, 2005)

For the maximum CGV requirement, the gamut volume is present in the CIE Lab color space. By matching the white point setting, utilizing Eq. (2-16), the color gamut can be designed by the relative luminances of four-primary. In addition, the CGV can be calculated by the equation:

$$CGV = \iiint G(L^*, a^*, b^*) dL^* da^* db^* \quad (2-20)$$

The color gamut volume is calculated in CIELAB color space when changing Y_c value, which is plotted in Fig. 2-6 from which the maximum gamut volume of 1.61×10^6 at $Y_y = 0.37$ can be derived.

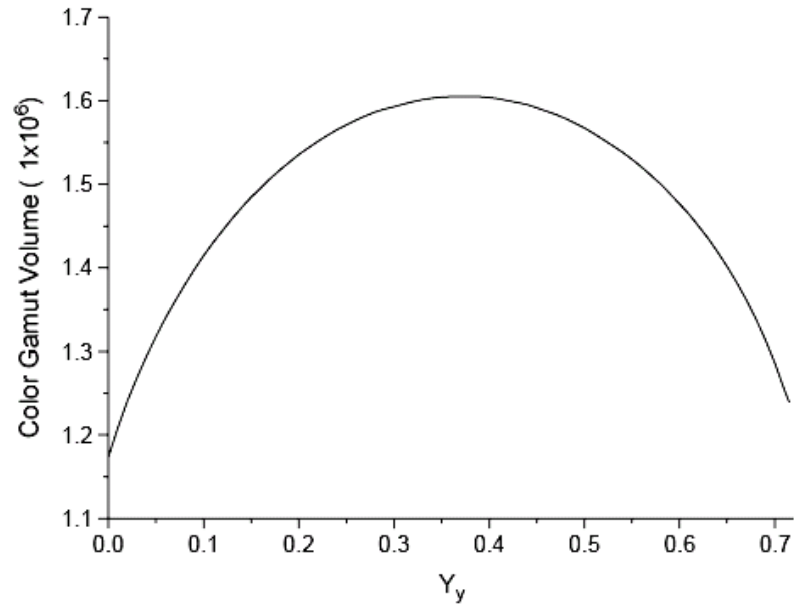


Fig. 2-6. The CGV (ΔE^*ab^3) of four-primary display plotted against Y_y (S. Wen, *Displays*, 26, pp. 171-176, 2005)

With these two proposed criteria, the four-primary display gamut can be achieved for its preferred application. Since the two criteria have two different settings, finally, Wen concluded that, in practice, the design of the relative primary luminances may be a compromised result of the two additional requirements. However, the criteria perform the largest CGV and maximum display luminance, but they do not consider the input CGV. So it may be not a suitable design for color reproduction.

2.3 Proposed method

Although the larger CGV can yield more colors, the mapping with input encoded CGV is

another key factor affecting the display color reproduction performance. Some paper [26] provides the metrics to judge the gamut volume of display, which depicts that the gamut volume characteristics is judged with the input encoding CGV. With this concept, the proposed new criterion is taking the input color gamut into account, which is the maximum intersectional CGV.

Consequently, this thesis refers to the Wen's method, with the maximum white point luminance requirement and adds the maximum input CGV intersection requirement. The method of designing the four-primary color gamut for reproducing maximum input encoded color was proposed. It compromised with the efficiency of maximum luminance, and performed the best gamut mapping resulted from input signal.

A four-primary-LED backlight in FS-FC LCDs was constructed to verify the proposed method, will be introduced in next chapter. The four primaries are red, green, blue, and cyan, denoted in R, G, B, and C separately. To meet the white point, the forward model modified from Eq. (2-13) is shown as follows:

$$\begin{bmatrix} X_w \\ Y_w \\ Z_w \end{bmatrix} = \begin{bmatrix} X_R & X_G & X_B & X_C \\ Y_R & Y_G & Y_B & Y_C \\ Z_R & Z_G & Z_B & Z_C \end{bmatrix} \begin{bmatrix} R \\ G \\ B \\ C \end{bmatrix} \quad (2-21)$$

The backward model of the relative luminance of four primaries modified from Eq. (2-16) is shown as follows:

$$\begin{bmatrix} Y_r \\ Y_g \\ Y_b \end{bmatrix} = \begin{bmatrix} \frac{x_r}{y_r} & \frac{x_g}{y_g} & \frac{x_b}{y_b} \\ 1 & 1 & 1 \\ \frac{z_r}{y_r} & \frac{z_g}{y_g} & \frac{z_b}{y_b} \end{bmatrix}^{-1} \begin{bmatrix} \frac{x_w}{y_w} - \frac{x_c}{y_c} Y_c \\ 1 - Y_c \\ \frac{z_w}{y_w} - \frac{z_c}{y_c} Y_c \end{bmatrix} \quad (2-22)$$

In addition, to consider the available luminance of each LED Y_{rm} , Y_{gm} , Y_{bm} , and Y_{cm} , the designed maximum efficiency of four LEDs, η_{max} , modified from Eq. (2-19) is defined as:

$$\eta_{\max}(Y_c) = \text{Min} \left\{ \frac{Y_{rm}}{Y_r} = \frac{Y_{gm}}{Y_g} = \frac{Y_{bm}}{Y_b} = \frac{Y_{cm}}{Y_c} \right\} \quad (2-23)$$

According to the calculated result of Eqs. (2-22) and (2-23), the maximum white point requirement can be achieved by the specific relative luminance of four primaries. The proposed maximum input CGV intersection requirement which is calculating the CGV intersection with input CGV in the CIELAB color space. The test input CGV, the sRGB color space [27] and the “real world surface color” gamut by pointer [28], will be introduced in next section. Then, the 3D color gamut visualization and the intersectional CGV calculating simulation will be introduced in next chapter.

In summary, the design flow of proposed method is shown in Fig. 2-7. First, the measurement data of four-primary color should be made to build a color database. Then, start designing the relative luminance of each primary. The first step is to meet the basic white point requirement by referring to the input color white point. Second, consult with the measurement database, the maximum available ratio also be calculated. With the maximum white point luminance design, the initial four-primary CGV can be determined by the relative luminance setting. Finally, the input CGV is taken to compare with the initial four-primary CGV. The maximum intersectional CGV will be found by shift-adjusting the initial setting. As a result, the new relative luminance setting decides the final four-primary CGV.

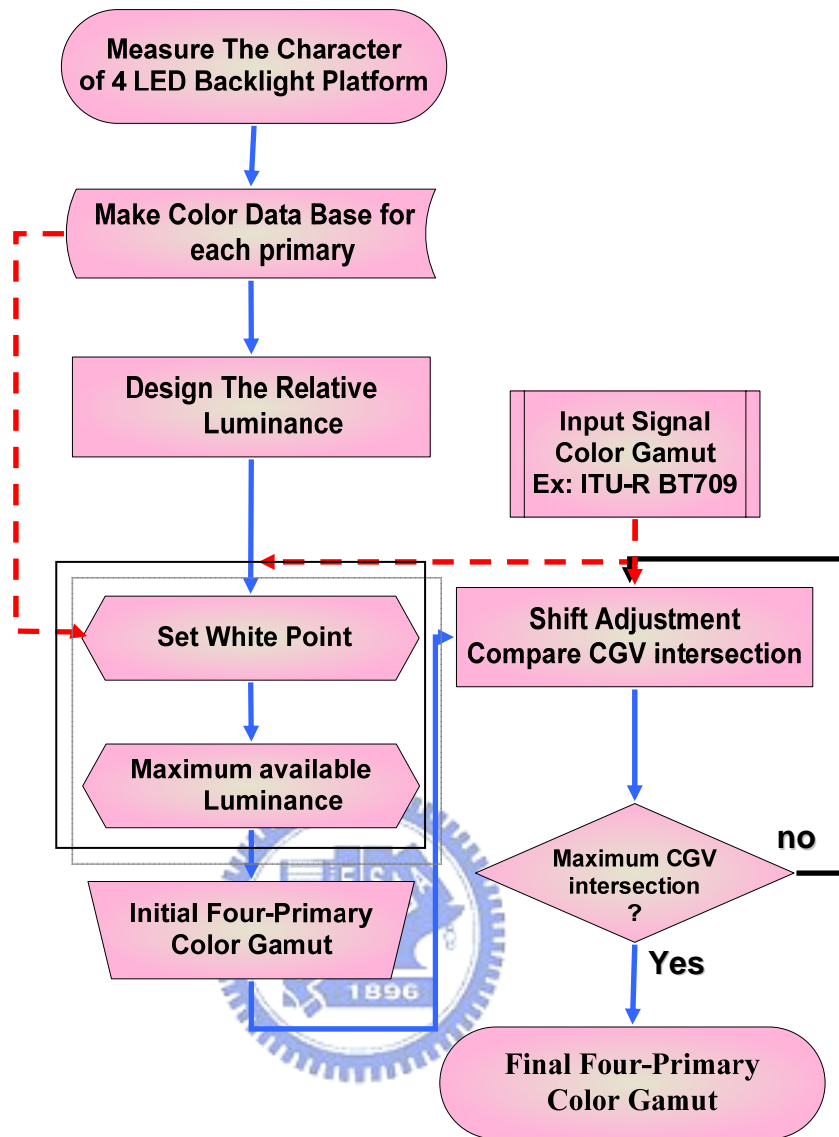


Fig. 2-7. The design flow of proposed method

2.4 Test input color gamuts

For the requirement of maximum input CGV intersection, the test color gamuts here, are the standard RGB (sRGB) color space and the “real world surface color”. The sRGB adopt the HDTV standard and is widely used in most monitor gamut management. Furthermore, the real surface database collected by pointer contains most of the colors that people can see in the real world.

2.4.1 Standard RGB color space (sRGB)

In 1996, Hewlett-Packard and Microsoft proposed a standard color space, sRGB, for the usage on monitors, printers, and the Internet. The aim of this color space was to complement the current color management strategies by enabling a third method of handling color in the operating system and device drivers. The sRGB is a single default color space acting as a bridge provides the good quality and backward compatibility with unambiguous and efficient transmission. Nowadays, the sRGB color space has been standardized by the International Electrotechnical Commission (IEC) as IEC 61966-2-1 in 1999 [29]. Such a standard can dramatically improve the color fidelity in the desktop environment

The three major factors of the sRGB standard are the colorimetric RGB definition, the equivalent gamma value of 2.2 and the well-defined viewing conditions, along with a number of secondary details necessary to enable the clear and unambiguous communication of color.

The sRGB standard used the ITU-R BT.709-2 reference primaries and the CIE standard illuminant D_{65} reference white. The ITU-R BT.709-2 defined the parameter values of the HDTV standards for production and international program exchange. The primaries and reference white of sRGB standard are given in Table 2-1.

Table 2-1 Parameters of sRGB chromaticities

CIE chromaticities for ITU-R BT.709 reference primaries and CIE standard illuminant				
	Red	Green	Blue	D65
x	0.6400	0.3000	0.1500	0.3127
y	0.3300	0.6000	0.0600	0.3290
z	0.0300	0.1000	0.7900	0.3583

Additionally, the standard adopted the transfer function (gamma 2.2) of typical CRTs. Gamma is the non-linearity of the electro-optical radiation transfer function of CRTs; This transfer function describes how much luminance results from voltages applied to the CRT, and often expressed by a mathematical exponential power function parameter.

After defining the parameters of colorimetry, the sRGB color space is designed to match typical home and office viewing conditions rather than the darker environment typically used for commercial color matching. The viewing environment descriptions contain all the necessary information to provide conversions between the standard and target viewing environments, as shown in Table 2-2:

Table 2-2 Parameters of sRGB viewing environment

sRGB viewing environment Parameters	
Condition	sRGB
Luminance level	80 cd/m ²
Illuminant White	$x = 0.3127, y = 0.3291$ (D65)
Image surround	20% reflectance
Encoding Ambient Illuminance Level	64 lux
Encoding Ambient White Point	$x = 0.3457, y = 0.3585$ (D50)
Encoding Viewing Flare	1.0%
Typical Ambient Illuminance Level	200 lux
Typical Ambient White Point	$x = 0.3457, y = 0.3585$ (D50)
Typical Viewing Flare	5.0%

2.4.2 Real-world surface colors gamut

In 1980, Pointer published an article titled “the gamut of real surface colours”, which collected 4089 measured surface color patches data enclosing most of the color in the real world. In this article all the data have been calculated using CIE Standard Illuminant C. The color patches contained the follows:

- (1) Munsell Color-Cascade (non-fluorescent)
- (2) Surface color objects measured by Trussel
- (3) DuPont paint samples
- (4) Graphic arts spot colors

As show in Fig. 2-8, the measurement color data was plotted in the CIE1931 xy chromaticity diagram. In addition, the data were converted into CIELAB coordinates, sorted into groups according to the hue angle, h_{ab} , and then represented as plots of lightness, L^* , as a function of chroma, C_{ab}^* . Similar calculations were made using the equivalent CIELUV coordinates. Both of these two coordinates collection used the convex hull, the smallest polygon that enclosed the sets of data to surround all these color data as a real-world surface color gamut.

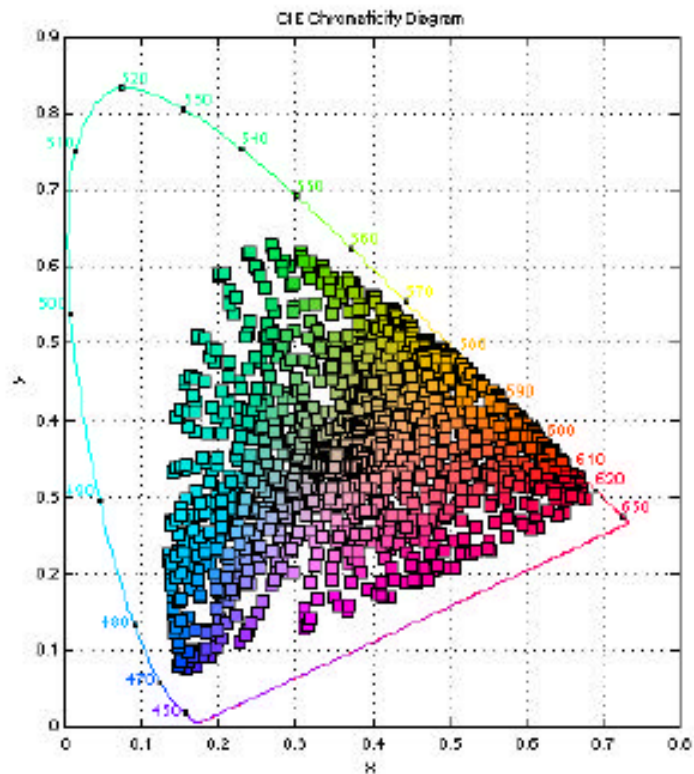


Fig. 2-8 The Pointer color gamut in CIE xy chromaticity diagram



This thesis used the sRGB and real-world surface color gamut in the CIELAB coordinate as input colors to evaluate the CGV setting of the four-primary LED backlight. Therefore, through the quantitatively evaluation of two input color gamuts, the four-primary gamut was able to represent the color chart with as much color fidelity as possible.

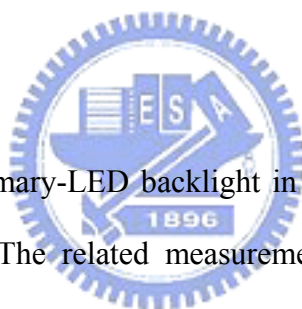
Chapter 3

Experiment and Simulation

This chapter has been divided into two sections: experiment and simulation. The experiment section includes four-primary-LED backlight platform, measurement equipment, and the measurement data, which will be firstly described for establishing a color database. In the simulation section, the simulation method for evaluating the gamut characteristic will be described.

3.1 Experiment

In this section, a four-primary-LED backlight in FS-FC LCDs has been constructed to verify the proposed method. The related measurement equipment and measurement data would be shown later.



3.1.1 Four-primary-LED backlight platform

The four-primary-LED backlight platform, as shown in Fig. 3-1, was composed of an optical cavity, a constant-current driving board, and a Field-programmable gate array (FPGA) control board. These parts would be introduced separately.

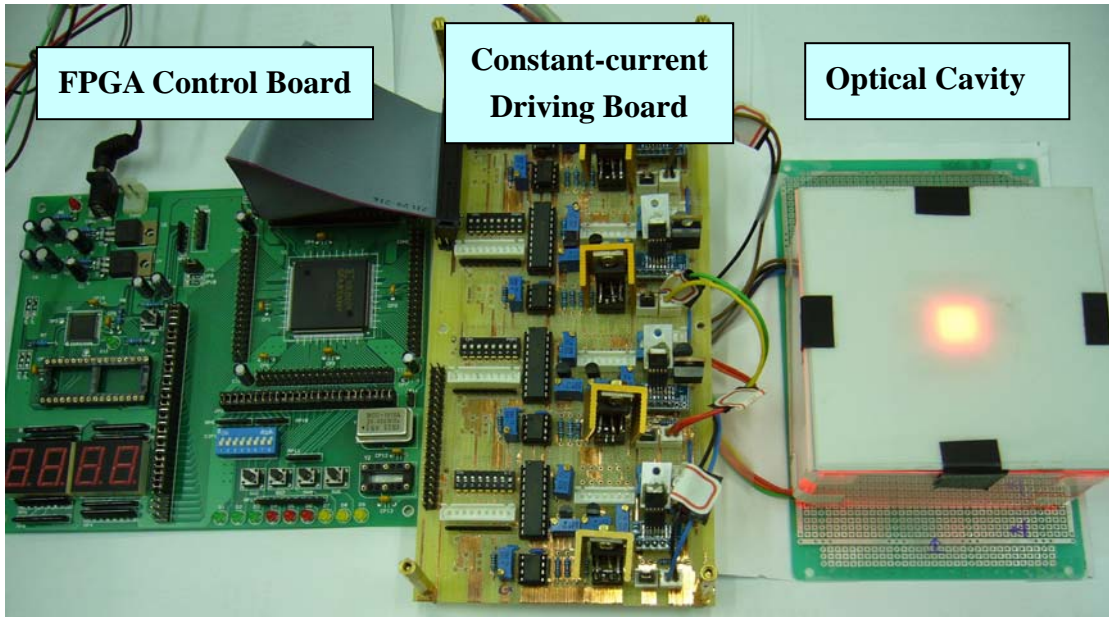


Fig. 3-1. The photo of four-primary-LED backlight platform, which included (a) a optical cavity, (b) a constant-current driving board, and (c) FPGA control signal board

The optical cavity, a sample of LED-Direct-Backlight, which was composed of four high flux LEDs i.e. Luxeon Star LEDs. A set of diffusers were covered on the four LEDs cavity. The main target was to mix the four-primary colors to obtain the best brightness and color uniformity in the center of the diffusers. The optical cavity and specifications of the selected LEDs from LUMINLEDS Corporation are shown in Fig. 3-2, where the peak wavelengths of red, green, blue, and cyan primaries were 625nm, 530nm, 470nm, and 505nm, respectively.

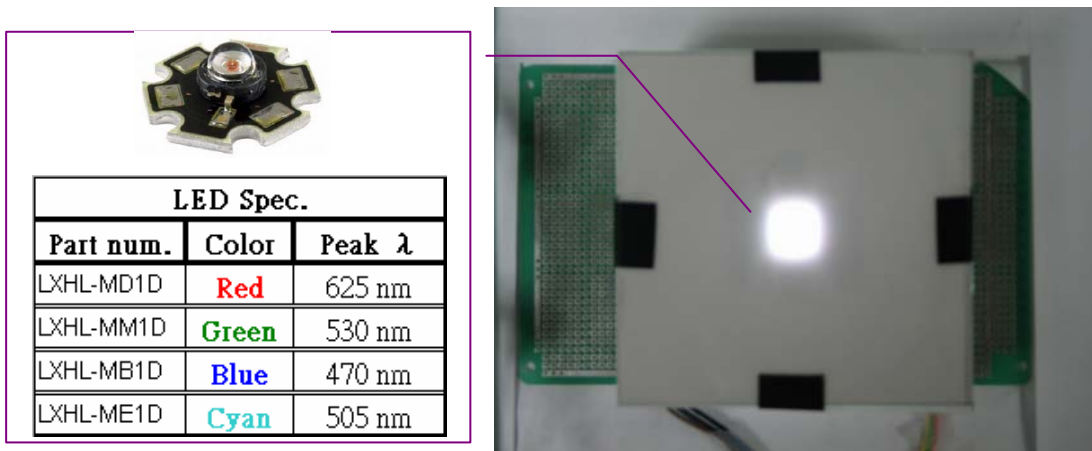


Fig. 3-2. The photo of simple optical cavity and the correlative specification of LED

The constant-current driving board designed to provide the constant current for each LED was expecting for the uniform color mixing result. As shown in Fig. 3-3, the circuit board was divided into four similar parts, and each part deriving one specific LED. The digital switch monitored the current which drives the LEDs, and the digital values were coded on eight bits digital/analog converter (DAC) resulting in 256 digital values. Moreover, the other circuits aided the LED driving IC providing different constant currents by the setting of each digit count.

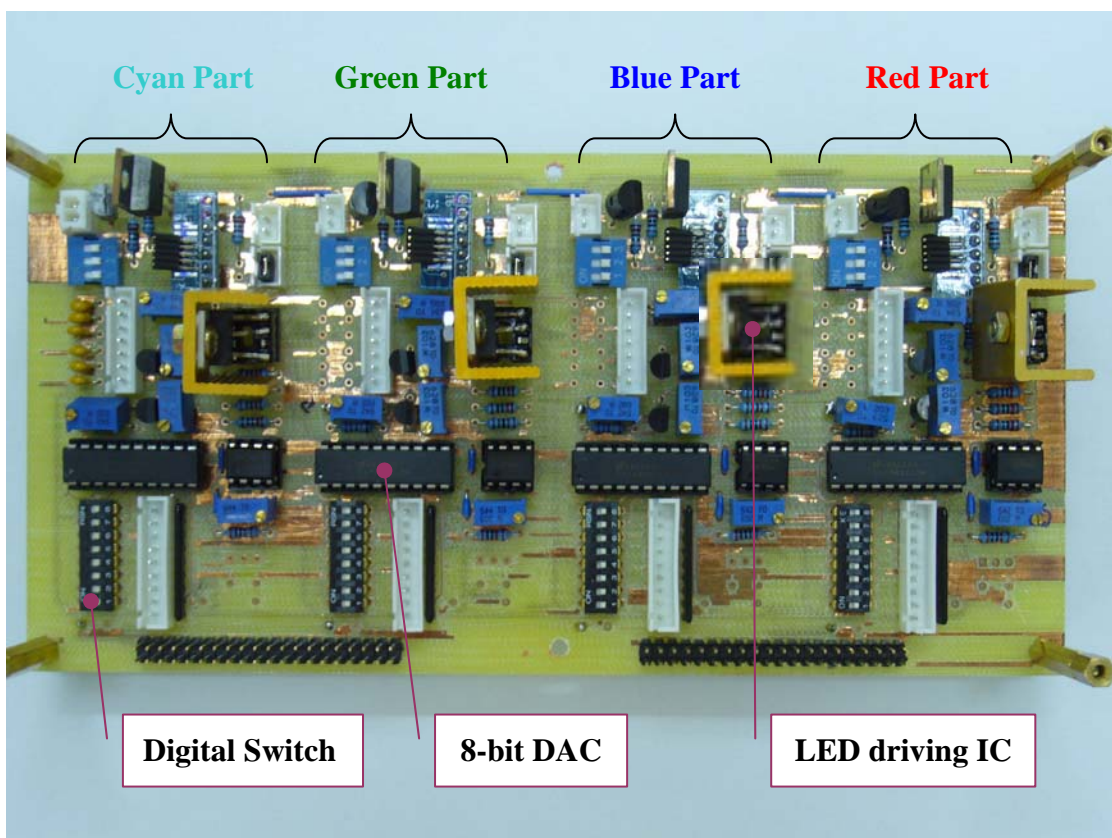


Fig. 3-3. The photo of constant-current driving board and its description

The FPGA control board produced the time-sequential signal allowing the switching of the driving current for each LED. This board was connected to the electronic driving board. By the Verilog coding, the digital count and the timing signal has been provided for each LED.

3.1.2 Measurement equipment

The instrument used to realize the measurements was the Conoscope, as shown in Fig. 3-4. The Conoscope has different applications: luminance vs. viewing direction, chromaticity vs. viewing direction, response time, flicker-analysis, lateral homogeneity, interactive viewing cone analysis, and electro-optical characterization, etc.



Fig. 3-4. The photo of Conoscope

In this thesis, the interesting function is the ability of the Conoscope to realize the measurements of the color coordinates (x, y) and tristimulus on our sample backlight. In the Conoscope, the luminous information of measurement sample is sent to two different devices, as shown in Fig. 3-5, totally independent in their work. The first device is the photometer with the CCD camera, which allows the measurement of the color coordinates. The results of the experiments are displayed on the computer linked to the Conoscope. The second device is the spectrometer, which provides more accurate spectrum measurement. The main function of the spectrometer is to measure the wavelength of the light produced by the studied sample. Additionally, the tristimulus and CIE coordinates was calculated by this function.

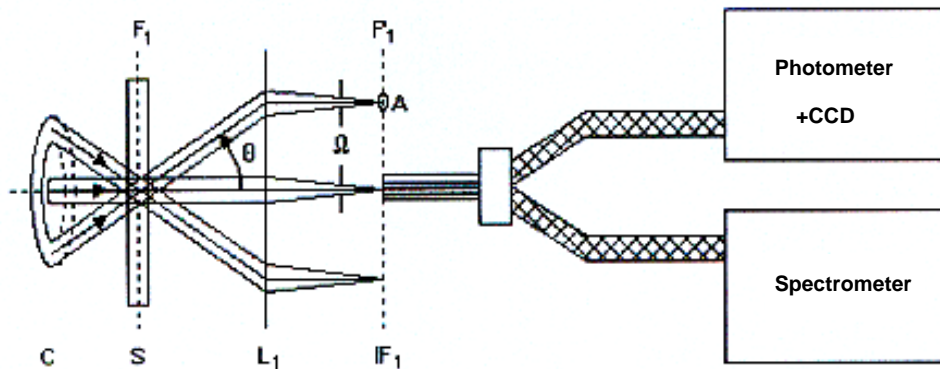


Fig. 3-5. The luminous information path in Conoscope

The Conoscope is based on the conoscopic method. As shown in Fig. 3-6, a cone of elementary parallel light beams C , which is transmitted by a sample S that is located in the front of focal plane of the lens L_1 , is collected simultaneously over a large solid angle by the lens L_1 . A pattern IF_1 is generated in the rear focal plane F'_1 of the lens L_1 by the transform lens. The intensity of each area element corresponds to the intensity of one elementary parallel beam with a specific direction of light propagation. In the pattern IF_1 , the directional intensity distribution of the cone of elementary parallel light beams C is transformed into a two-dimensional distribution of light intensity and color with each location in the pattern corresponding to exactly one direction of light propagation (θ , ϕ).

For the CCD detector, a second optical system L_2 optionally projects the conoscopic figure IF_1 on a two dimensional detector array for evaluation of the spatial intensity distribution, which corresponds to the directional intensity distribution of the light emerging from the measuring spot on the sample.

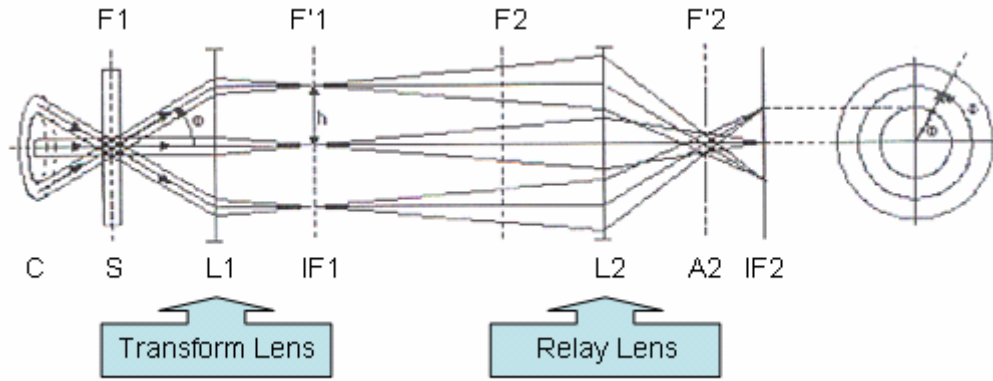


Fig. 3-6. The principle diagram of Conoscope

3.1.3 Measurement data

The specifications of each LED were measured by Conoscope Spectrometer. The calculated color gamut was about 131% of NTSC color gamut in 1931 CIE xy chromaticity diagram and 147% of NTSC color gamut in CIE 1976 UCS diagram, as shown in Table 3-1.

Table 3-1 LED specifications and measurement data

LED Spec.		Measurement Data			
Part num.	Color	Peak λ	x	y	Calculate Data
LXHL-MD1D	Red	625 nm	0.70	0.30	CIE xy color gamut
LXHL-MM1D	Green	530 nm	0.16	0.71	
LXHL-MB1D	Blue	470 nm	0.14	0.05	CIE u'v' color gamut
LXHL-ME1D	Cyan	505 nm	0.08	0.54	

The four-primary color gamut compared to other standard color gamuts in CIE 1976 UCS diagram is shown in Fig. 3-7 from which the designed color gamut was sufficient to reproduce the standard color gamut input.

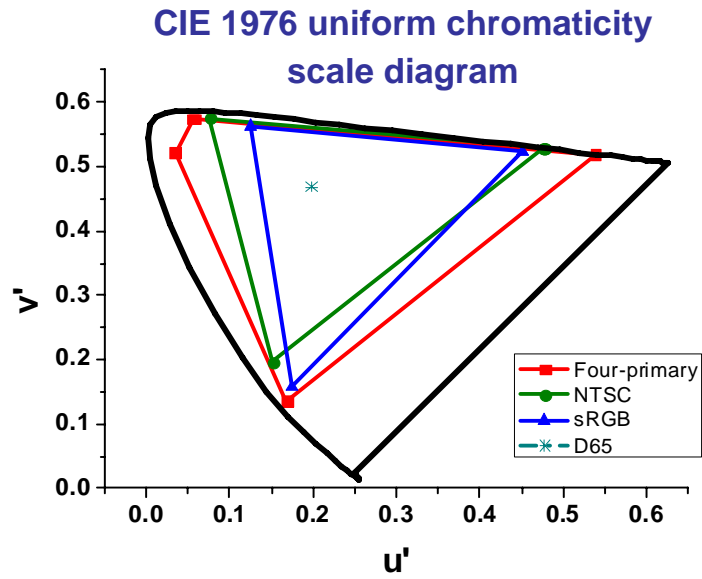


Fig. 3-7. Four-primary color gamut compared with standard color space in CIE 1976 UCS diagram

In addition, the database of these LEDs was measured by the adjustable current driving circuit, as shown in Fig. 3-8. The luminances of four LEDs, which denoted in R, G, B, and C, are almost linear functions of the digital count. The measurement data are also plotted in CIE 1931 chromaticity diagram, as shown in Fig. 3-9. The coordinates are not varied with the digital count. Therefore, the database of these LEDs can be applied to the color gamut evaluation.

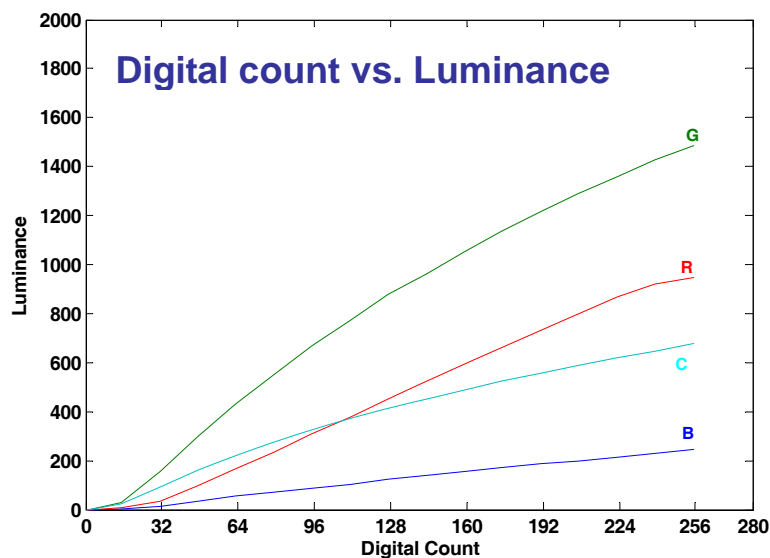


Fig. 3-8. Luminance of each primary plotted against digital count of control circuit

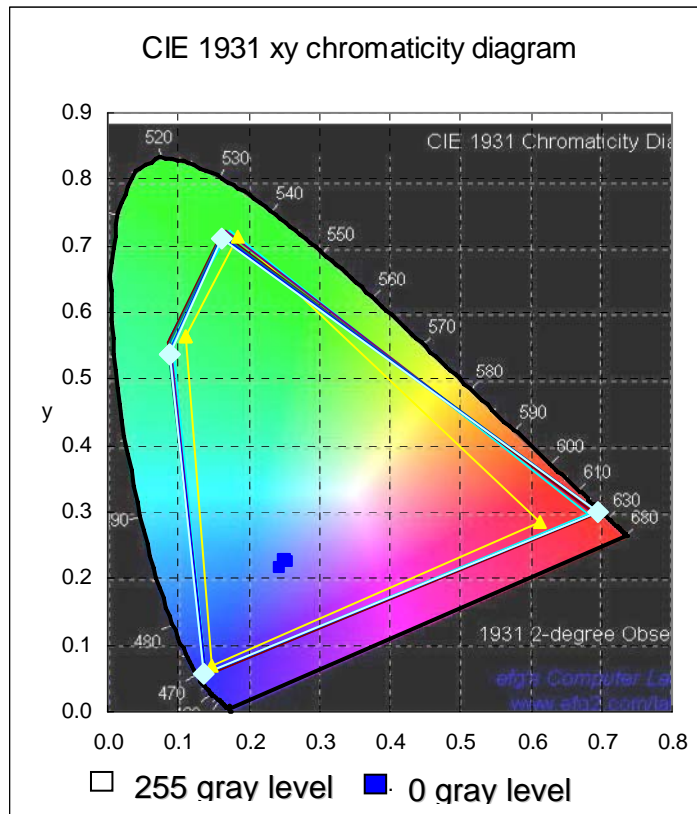


Fig. 3-9. The plot of different digital count (divided into 8 levels) in the CIE xy chromaticity diagram



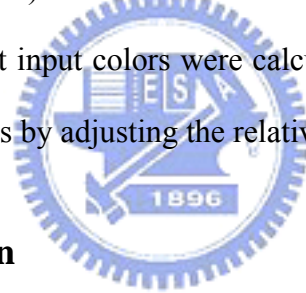
3.2 Simulation

The simulation includes the analysis of numerical parameters that above mentioned and the gamut visualization in three dimensions performed to observe the gamut intersection. In addition, the q-hull algorithm was also introduced in this section.

3.2.1 Numerical analysis

There are several parameters need to be simulated, included the max efficiency η_{\max} , maximum four-primary CGV, and the intersectional CGV (with input color gamut).

As mentioned before, the four-primary would produce a set of combinations through different relative luminance setting. Therefore, the max efficiency η_{\max} was calculated by satisfying Eqs. (2-22) and (2-23). The maximum four-primary CGV and the intersectional CGV of four primaries and test input colors were calculated by Eq. (2-20), and both of them try to meet the maximum values by adjusting the relative luminance.



3.2.2 Gamut visualization

As mentioned earlier, the color gamut is usually visualized and processed in the CIELAB color space. Because there are lots of set colors, the visualization of the gamut volume should use a convex hull to enclose all these data. The convex hull is the smallest polygon that enclosing all sets of data. As shown in Fig. 3-10, the set of color data in CIELAB color space are denoted, S , and the convex hull is the set which contain all the data denoted, $CH(S)$.

There are many algorithms for solving the convex hull problem. This thesis used the q-hull algorithm for the high speed approach, and it would be introduced later.

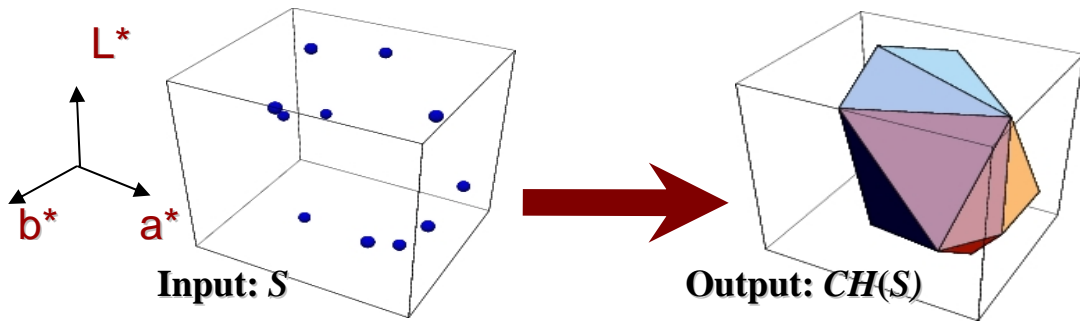


Fig. 3-10. The concept of convex hull in gamut visualization

3.2.3 Q-hull algorithm

The q-hull algorithm is the abbreviation of quick hull, which can provide the fast process in practice. The method is similar to the quick sort algorithm, the average time complexity is $O(n \log n)$.

The simple illustration of q-hull algorithm method is shown in Fig. 3-11. There are a set of points in the diagram. First, two points P_1 and P_2 are chosen and a line is drawn dividing the set of points in two parts i.e. X_1 , X_2 . In X_1 part, the P_3 is chosen to compose of the largest triangle area of $P_1P_2P_3$. Further, keep doing the same procedure, in the end; the final convex hull will be given.

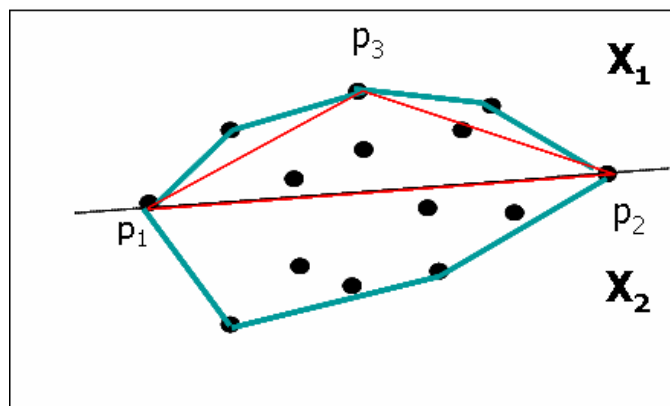


Fig. 3-11. The simple illustration of q-hull algorithm method

Chapter 4

Results & Discussion

The simulations of two input color gamuts, sRGB and real surface color gamut, are demonstrated and compared with the experimental data. Two commonly considered criteria and our proposed one will be examined in both input cases. These criteria include maximum white point luminance, maximum four-primary CGV and maximum intersectional CGV. The CGV is calculated in CIELAB space and depicted in three dimensions for direct comparison and clear visualization.

4.1 sRGB color gamut as the input

The input color gamut is sRGB color space, which was introduced in section 2.4.1, and the results from fulfilling of the three criteria will be shown separately.

4.1.1 Maximum white point luminance

The white point and the maximum available luminance of LEDs are required to meet the maximum white point luminance as proposed by Wen. For a standard ITU-R BT.709 (sRGB) input encoded color signal, the white point D65 decided by the maximum luminance and relative ratio of each primary is the starting point for defining the color gamut of a display. Using the measured database and Eq. (2-22), the white point shown in Table 2-1 can be achieved by different combinations of relative luminance setting. The varied Y_c was applied to Eq. (2-22), and plotted curve, as shown in Fig. 4-1, was resulted. Each vertical line in the diagram is under the white point requirement, e.g. when the relative luminance is setting at

vertical line 1, which is $Y_c=0.2$, $Y_r=0.289$, $Y_g=0.45$, and $Y_b=0.061$, the mixing result will agree with the D65 white point coordinates. It is noticed that the LED backlight reduces to three primaries for the cases of $Y_c=0$ and 0.63 . Because Y_c is the luminance of comprises of blue and green spectral components, the required luminance of blue and green primaries decrease as Y_c increases. On the other hand, the required luminance of red primary is increased with Y_c . Therefore, the varied Y_c lies on the range of two boundaries.

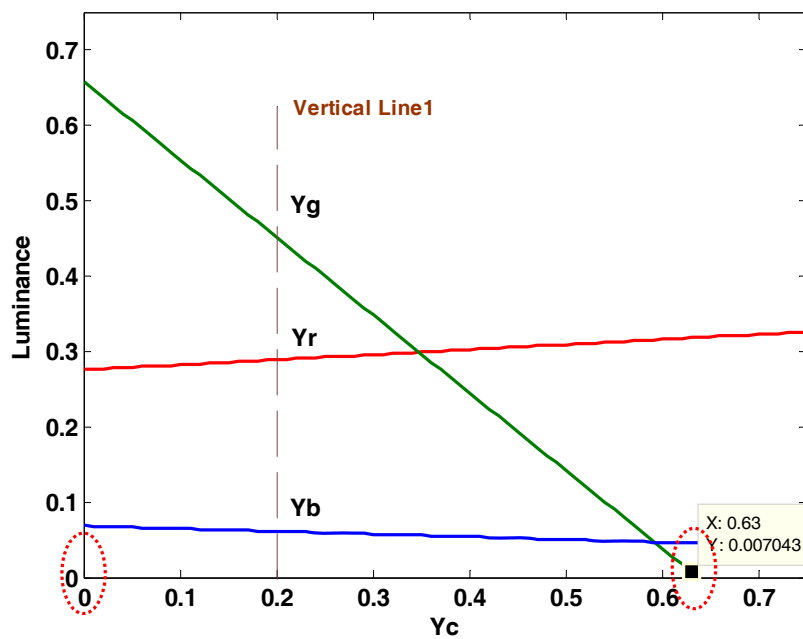


Fig. 4-1. Plots of luminances Y_r , Y_g , and Y_b as functions of Y_c under the white point requirement

In addition, if considered the available luminance ratio of each LED at the white point, the luminance ratios as functions of Y_c are shown in Fig. 4-2 by Eqs. (2-22) and (2-23). The minimum ratio is 0.9801 at $Y_c=0.2$ which is the maximum efficiency η_{max} defined by Eq. (2-23). The designed efficiency of four LEDs η is plotted in Fig. 4-3 by applying the varied Y_c to Eq. (2-23) for the comparison. As shown in Fig. 4-3, the maximum efficiency of 0.98 at $Y_c=0.2$ can be derived. Therefore, the initial four-primary color gamut with maximum white point luminance requirement is defined, when $Y_c=0.2$, $Y_r=0.289$, $Y_g=0.45$, and $Y_b=0.061$, respectively.

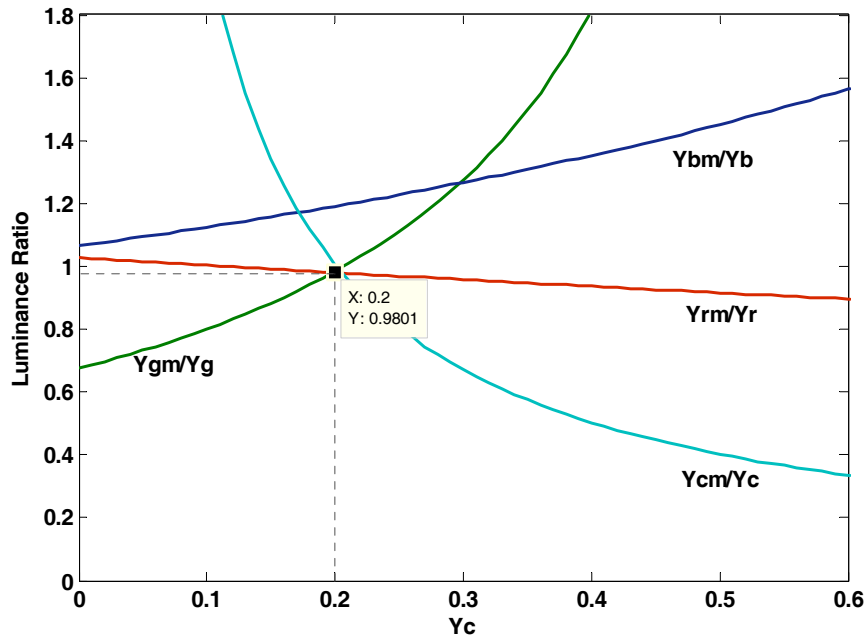


Fig. 4-2. Plots of luminance ratios Y_m/Y_r , Y_{gm}/Y_g , Y_{bm}/Y_b , and Y_{cm}/Y_c as functions of Y_c

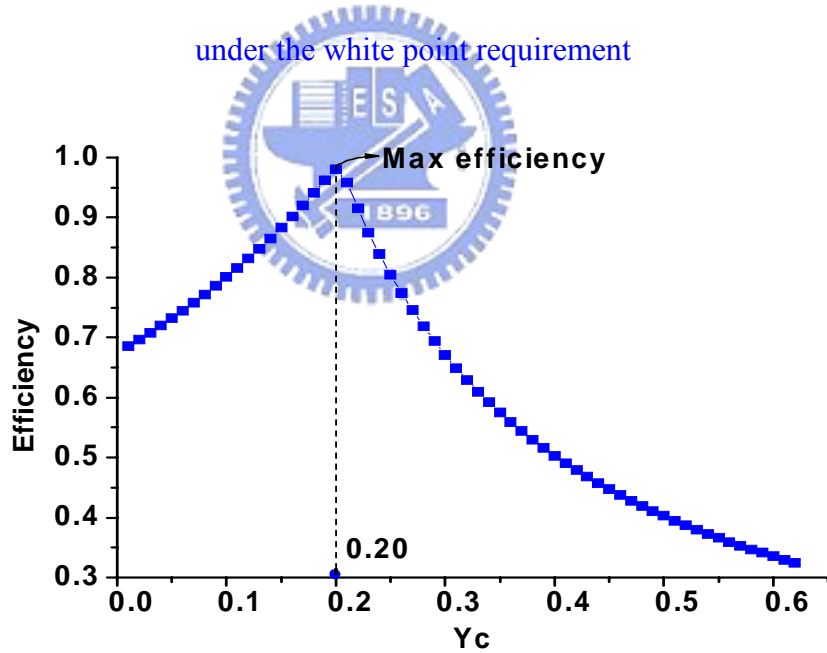


Fig. 4-3. The available LED efficiency plotted against Y_c under the sRGB gamut input

4.1.2 Maximum four-primary CGV

The maximum CGV of four-primary display was also considered in Wen's method. The CGV was calculated in CIELAB color space by Eq. (2-20) with the varied Y_c value, as shown

in Fig. 4-4. The maximum gamut volume of 1.7×10^6 at $Y_c=0.24$ can be derived. As a result, the maximum four-primary CGV with white point requirement is defined, when $Y_c=0.24$, $Y_r=0.291$, $Y_g=0.409$, and $Y_b=0.06$, respectively.

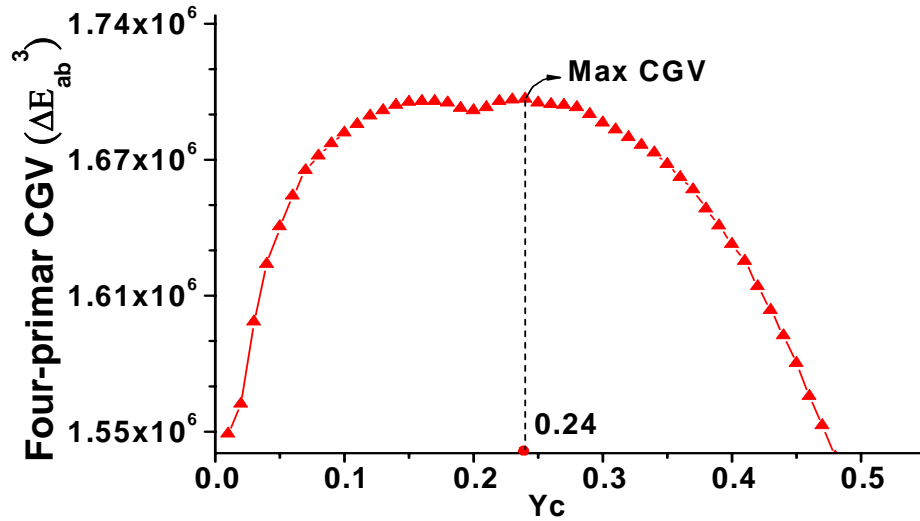


Fig. 4-4. The four-primary CGV plotted against Y_c under the sRGB gamut input

4.1.3 Maximum input CGV intersection

According to the design flow of proposed method in Fig. 2-7, the initial four-primary CGV was achieved by fulfilling of the maximum white point luminance requirement. In addition, the initial four-primary CGV with different relative luminance setting was compared with the input gamut. Therefore, the intersectional CGV of four-primary LED backlight and sRGB color gamut was also derived by Eq. (2-20). Then, the intersectional CGV plotted against the shifted Y_c value is shown in Fig. 4-5. Obviously, from this figure, the intersectional CGV value becomes larger when Y_c value is reduced. The maximum value is achieved when the initial Y_c value shift from 0.2 to 0.04. By using Eq. (2-22), the relative luminances are $Y_c=0.04$, $Y_r=0.278$, $Y_g=0.615$, and $Y_b=0.067$, respectively.

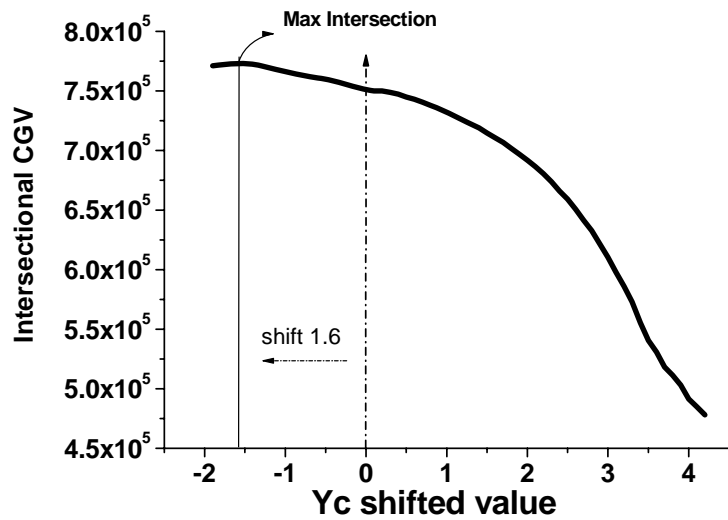


Fig. 4-5. Plot of intersectional CGV as a function of the shifted Y_c value under sRGB gamut input

In order to observe the color gamut intersection, the 3D CGV visualization of initial four-primary and sRGB color gamut were presented in CIELAB color space by q-hull algorithm simulation, as shown in Figs. 4-6 and 4-7. Furthermore, the intersectional CGV visualization by combining the two color gamut is shown in Fig. 4-8 from which some part of sRGB CGV is not included in the four-primary CGV.

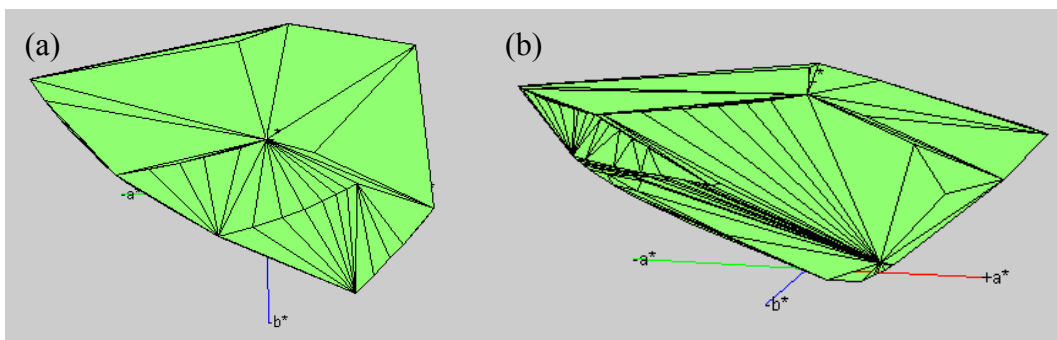


Fig. 4-6. 3D visualization of four-primary gamut in CIELAB color space with different angle of (a) top and (b) side view

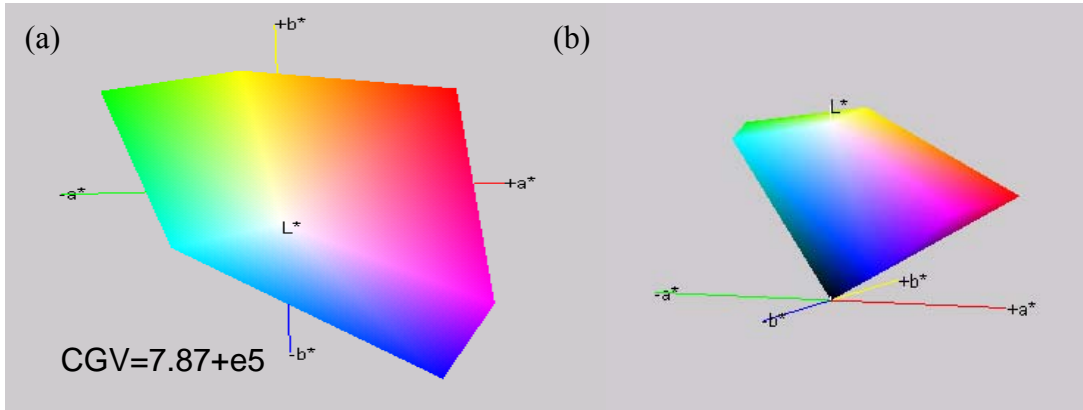


Fig. 4-7. 3D visualization of sRGB color gamut in CIELAB color space with different angle of (a) top and (b) side view

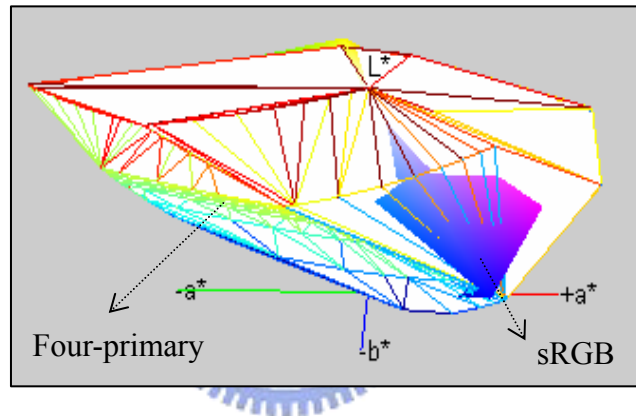


Fig. 4-8. 3D CGV Intersection of four-primary gamut and sRGB gamut

4.1.4 Summary

With sRGB color gamut as an input, the results of three criteria are performed by the value setting shown in Table 4-1. The relative luminance of each primary and the digital level setting were listed. Furthermore, the curves based on three criteria are plotted in Fig. 4-9 for the comparison.

Table 4-1 The relative luminance setting of each criterion with sRGB gamut input

Relative luminance		Y _r	Y _g	Y _b	Y _c
Max White Point Luminance	Ratio	0.289	0.45	0.061	0.2
	Level	255	254	209	248
Max CGV	Ratio	0.291	0.409	0.06	0.24
	Level	220	197	175	255
The Proposed Design	Ratio	0.278	0.615	0.067	0.04
	Level	180	255	168	36

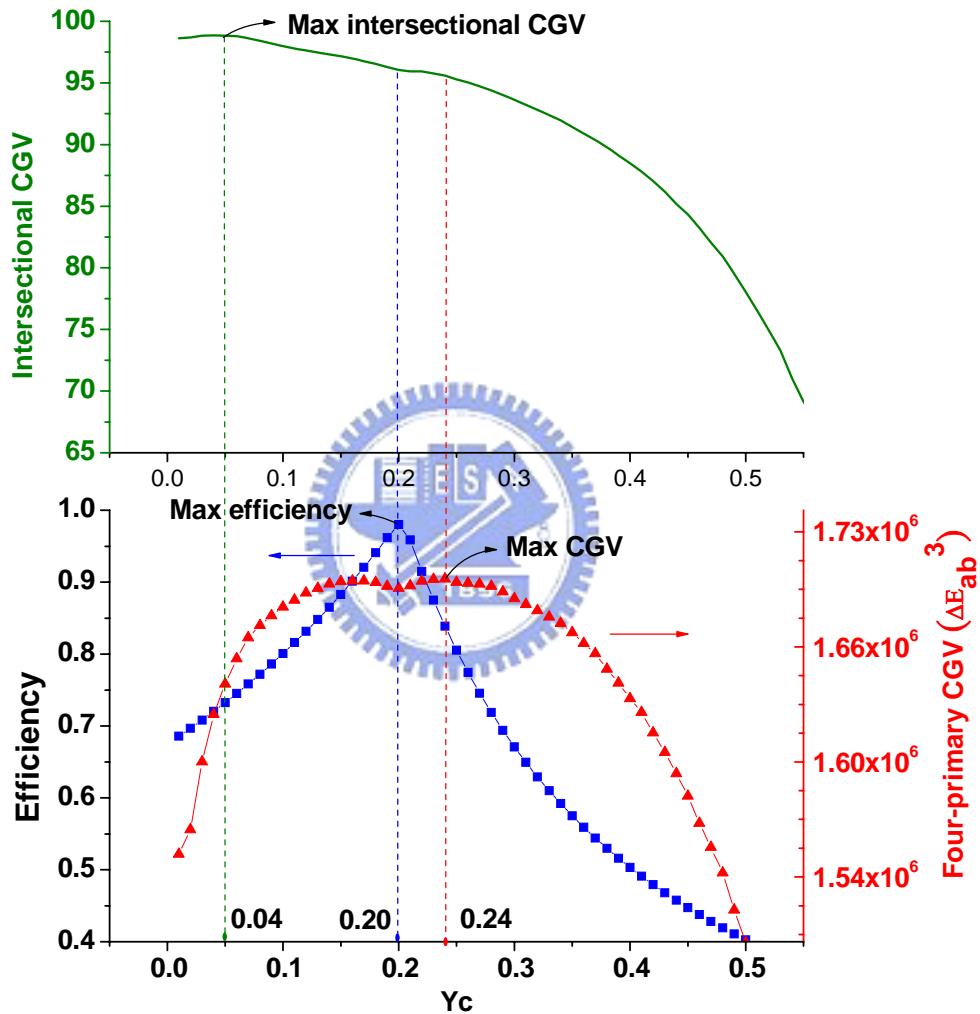


Fig. 4-9. Efficiency, four-primary CGV, and the intersectional CGV plotted against Y_c for comparison with sRGB gamut input

The comparisons of computed data based on three criteria including the maximum efficiency, four-primary CGV, and intersectional CGV, are shown in Table 4-2. The first row is the computed results of maximum white point luminance requirement at $Y_c=0.22$, the maximum efficiency is 0.98, the four-primary CGV is about 1.696×10^6 , and the

intersectional CGV is about 96.1 % of sRGB CGV. Then, the second row is the computed results of the maximum CGV requirement at $Y_c=0.24$, the maximum efficiency is 0.84, the four-primary CGV is about 1.7×10^6 , and the intersectional CGV is about 95.6 % of sRGB CGV. Furthermore, the third row is the computed results the maximum intersectional CGV requirement at $Y_c=0.04$, the maximum efficiency is 0.72, the four-primary CGV is about 1.626×10^6 , and the intersectional CGV is about 98.9 % of sRGB CGV. Obviously, each criterion has the largest value, which will be discussed in section 4.3.

Table 4-2 The compared result of each criterion

TEST INPUT	Criteria Used	Y_c	η_{max}	Four-primary CGV (ΔE_{ab}^3)	Intersectional CGV (with gamut input)
sRGB Color Space	Max White Point Luminance	0.20	0.98	1.696×10^6	96.1 % Input CGV
	Max CGV	0.24	0.84	1.702×10^6	95.6 % Input CGV
	The Proposed Design	0.04	0.72	1.626×10^6	98.9% Input CGV

With the three criteria settings, the LED backlight was set to achieve the white point of the display system and measured the color difference. As shown in Table 4-6, the measured color difference in $\Delta u'v'$ is lower than the minimum perceptible limit. ($0.005\Delta u'v'$). Consequently, the designed relative luminance is acceptable.

Table 4-3 The color difference with the reference white D65 in CIE 1976 UCS diagram of each criterion

criteria	result	$\Delta u'v'$ (with D65)
Max White Point Luminance		4.54×10^{-4}
Max CGV		4.407×10^{-3}
The Proposed Design		4.973×10^{-3}

4.2 Real surface color gamut as the input

The input color gamut is replaced with real surface color gamut which was introduced in section 2.4.2. Similar to last section, the results from fulfilling of the three criteria will be shown separately.

4.2.1 Maximum white point luminance

For a real surface color gamut, the white point C decided by the maximum luminance and relative ratio of each primary is the starting point for defining the color gamut of a display. Using the measured database and Eq. (2-22), the white point of illuminance C can be achieved by different combinations of relative luminance setting. The varied Y_c was applied to Eq. (2-22), and plotted curve, as shown in Fig. 4-10, was resulted. Each vertical line in the diagram is under the white point requirement, e.g. when the relative luminance sets at vertical line 1, which $Y_c=0.19$, $Y_r=0.295$, $Y_g=0.447$, and $Y_b=0.068$, the mixing result will agree with the illuminance C white point coordinates. It is also noticed that the LED backlight reduces to three primaries for the cases of $Y_c=0$ and 0.62. Because Y_c is the luminance of comprises of blue and green spectral components, the required luminance of blue and green primaries decrease as Y_c increases. On the other hand, the required luminance of red primary is increased with Y_c . Therefore, the varied Y_c lies on the range of two boundaries.

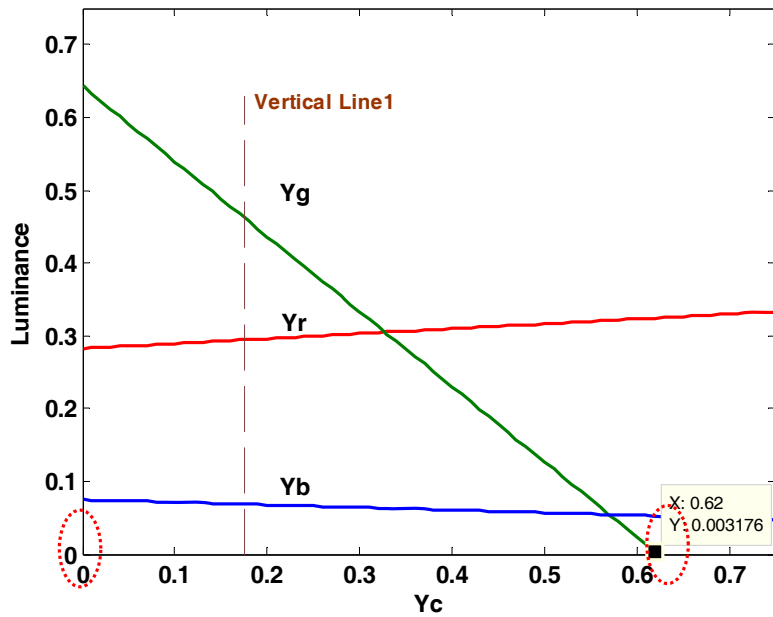


Fig. 4-10. Plots of luminances Y_r , Y_g , and Y_b as functions of Y_c under the white point requirement

In addition, if considered the available luminance ratio of each LED at the white point C, the luminance ratios as functions of Y_c are shown in Fig. 4-11 by Eqs. (2-22) and (2-23). The minimum ratio of 0.96 at $Y_c=0.19$ is the maximum efficiency η_{\max} defined by Eq. (2-23). Besides, the designed efficiency of four LEDs, η , is plotted in Fig. 4-12 by applying the varied Y_c to Eq. (2-23) for the comparison. As shown in Fig. 4-12, the maximum efficiency η_{\max} of 0.9598 at $Y_c=0.19$ can be derived. Thus, the initial four-primary color gamut with maximum white point luminance requirement is defined, when $Y_c=0.19$, $Y_r=0.295$, $Y_g=0.447$, and $Y_b=0.068$, respectively.

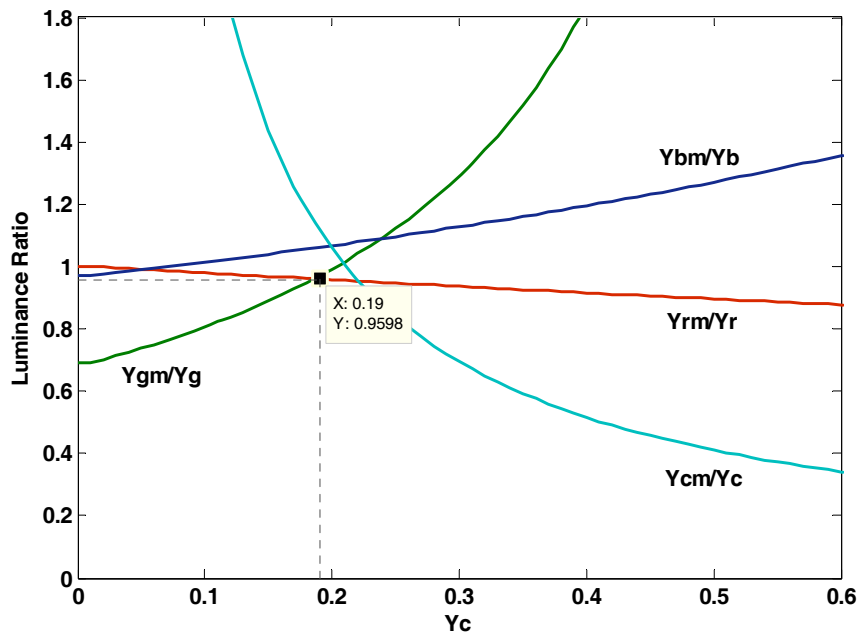


Fig. 4-11. Plots of luminance ratios Y_{rm}/Y_r , Y_{gm}/Y_g , Y_{bm}/Y_b , and Y_{cm}/Y_c as functions of Y_c under the white point requirement

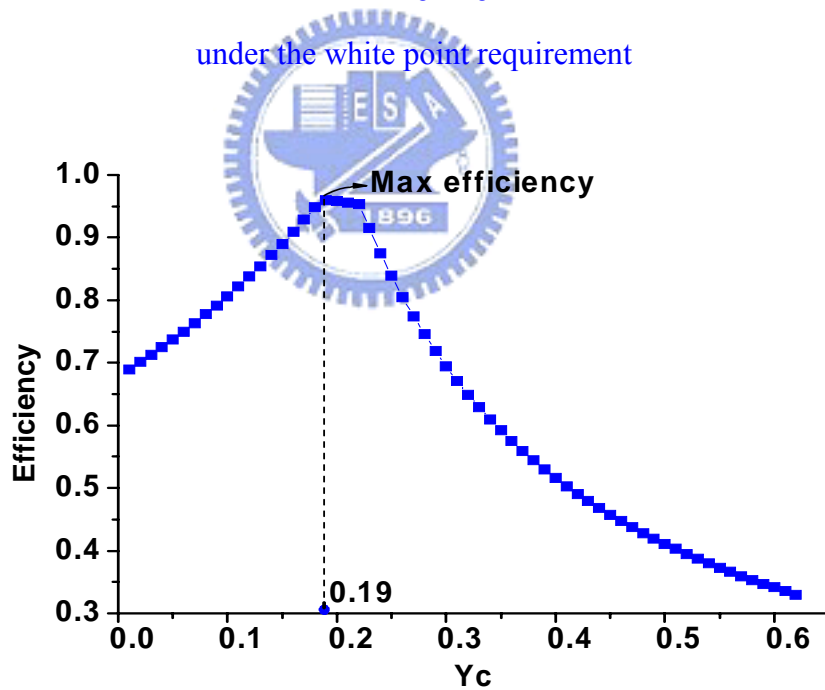


Fig. 4-12. The available LED efficiency plotted against Y_c under real surface gamut input

4.2.2 Maximum four-primary CGV

The maximum CGV of four-primary display was also considered in Wen's method. The

color gamut volume was calculated in CIELAB color space by Eq. (2-20) with varied Y_c value, as shown in Fig. 4-13. The maximum gamut volume of 1.69×10^6 at $Y_c=0.25$ can be derived. The maximum four-primary CGV with white point requirement is defined, when $Y_c=0.25$, $Y_r=0.299$, $Y_g=0.385$, and $Y_b=0.066$, respectively.

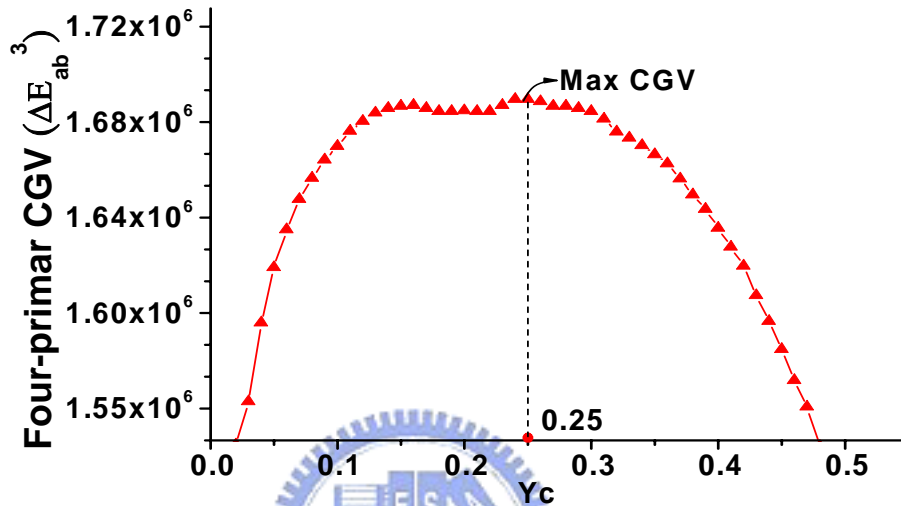


Fig. 4-13. The four-primary CGV plotted against Y_c under the real surface gamut input

4.2.3 Maximum input CGV intersection

According to the design flow of proposed method in Fig. 2-7, the initial four-primary CGV was achieved by fulfilling of the maximum white point luminance requirement. In addition, the initial four-primary CGV with different relative luminance setting was compared with the input gamut. The intersectional CGV of four-primary LED backlight and real surface color gamut was also derived by Eq. (2-20). Then, the intersectional CGV plotted against the shifted Y_c value is shown in Fig. 4-14. Obviously, the maximum value is achieved when Y_c from the initial value shift from 0.19 to 0.07. By using Eq. (2-22), the relative luminances are $Y_c=0.07$, $Y_r=0.287$, $Y_g=0.57$, and $Y_b=0.072$, respectively.

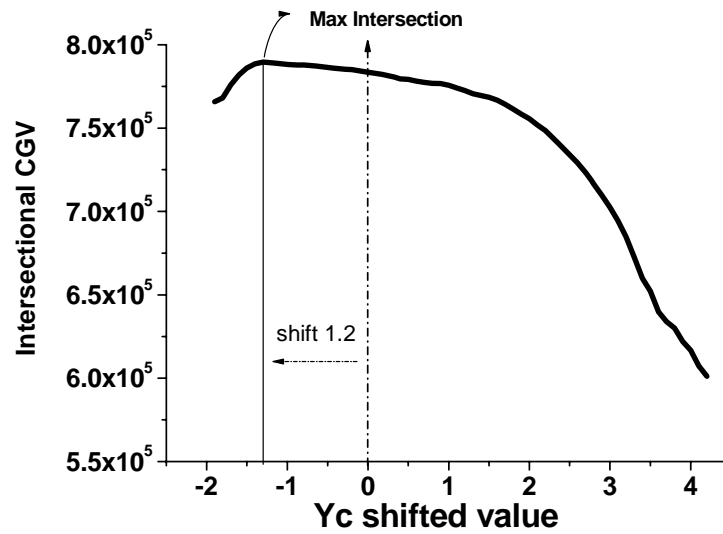


Fig. 4-14. Plot of intersectional CGV as a function of the shifted Y_c value under real surface gamut input

The 3D CGV visualization of initial four-primary and real surface color gamut were presented in CIELAB color space by q-hull algorithm simulation for the observation, as shown in Figs. 4-15 and 4-16. Besides, the intersectional CGV visualization by combining the two color gamuts is shown in Fig. 4-17 from which some part of real surface color gamut is not included in the four-primary color gamut.

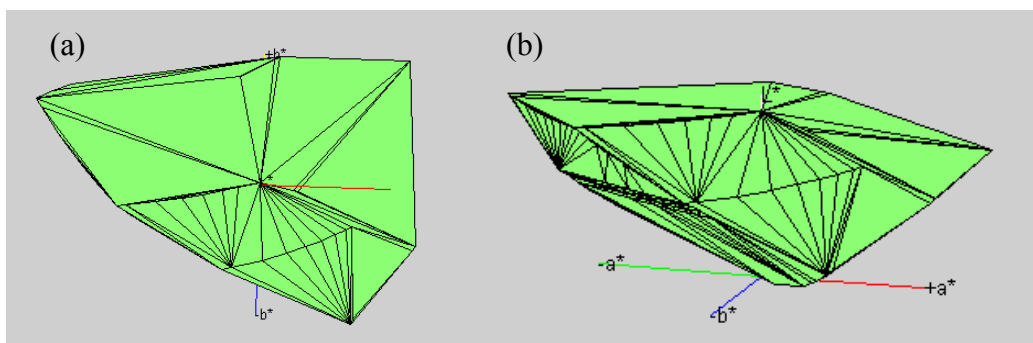


Fig. 4-15. 3D visualization of four-primary gamut in CIELAB color space with different angle of (a) top and (b) side view

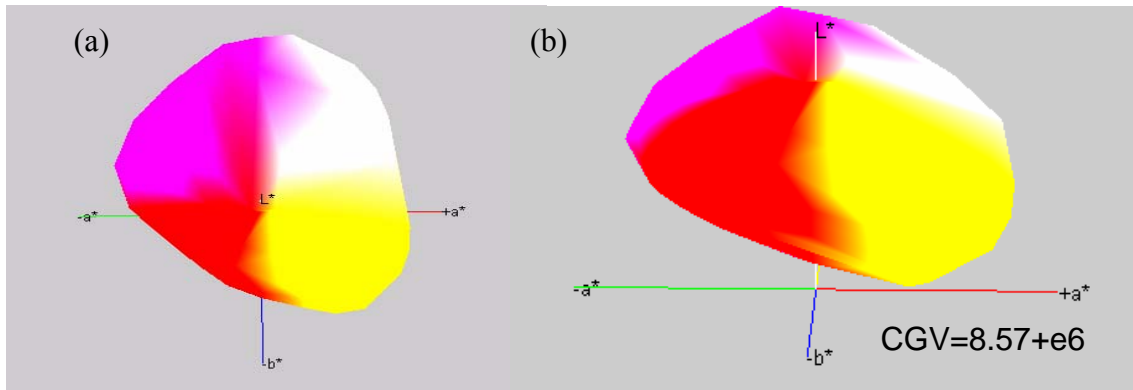


Fig. 4-16. 3D visualization of real surface color gamut in CIELAB color space with different angle of (a) top and (b) side view

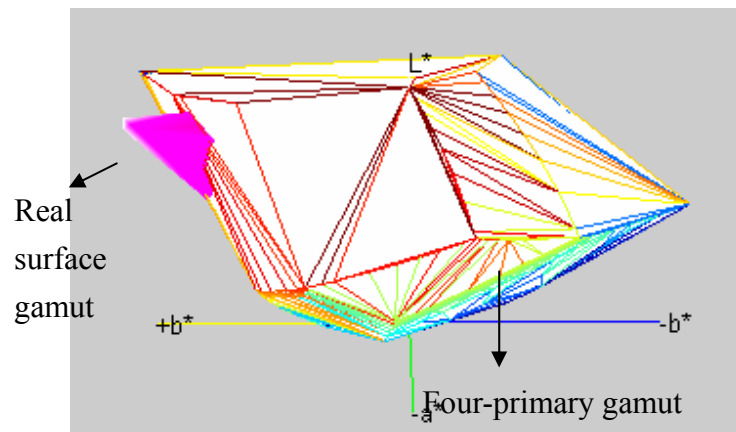


Fig. 4-17. 3D CGV Intersection of four-primary gamut and real surface color gamut

4.2.4 Summary

With the real surface color gamut as input, the three criteria are performed by the value setting shown in Table 4-4. The relative luminance of each primary and the digital level setting were listed. In addition, for the convenient comparison, the curves based on three criteria are plotted in Fig. 4-18.

Table 4-4 The relative luminance setting of each criterion with real surface gamut input

Relative luminance		Y _r	Y _g	Y _b	Y _c
Max White Point Luminance	Ratio	0.295	0.447	0.068	0.19
	Level	255	252	230	218
Max CGV	Ratio	0.299	0.385	0.066	0.25
	Level	225	190	195	255
The Proposed Design	Ratio	0.287	0.57	0.072	0.07
	Level	197	255	195	58

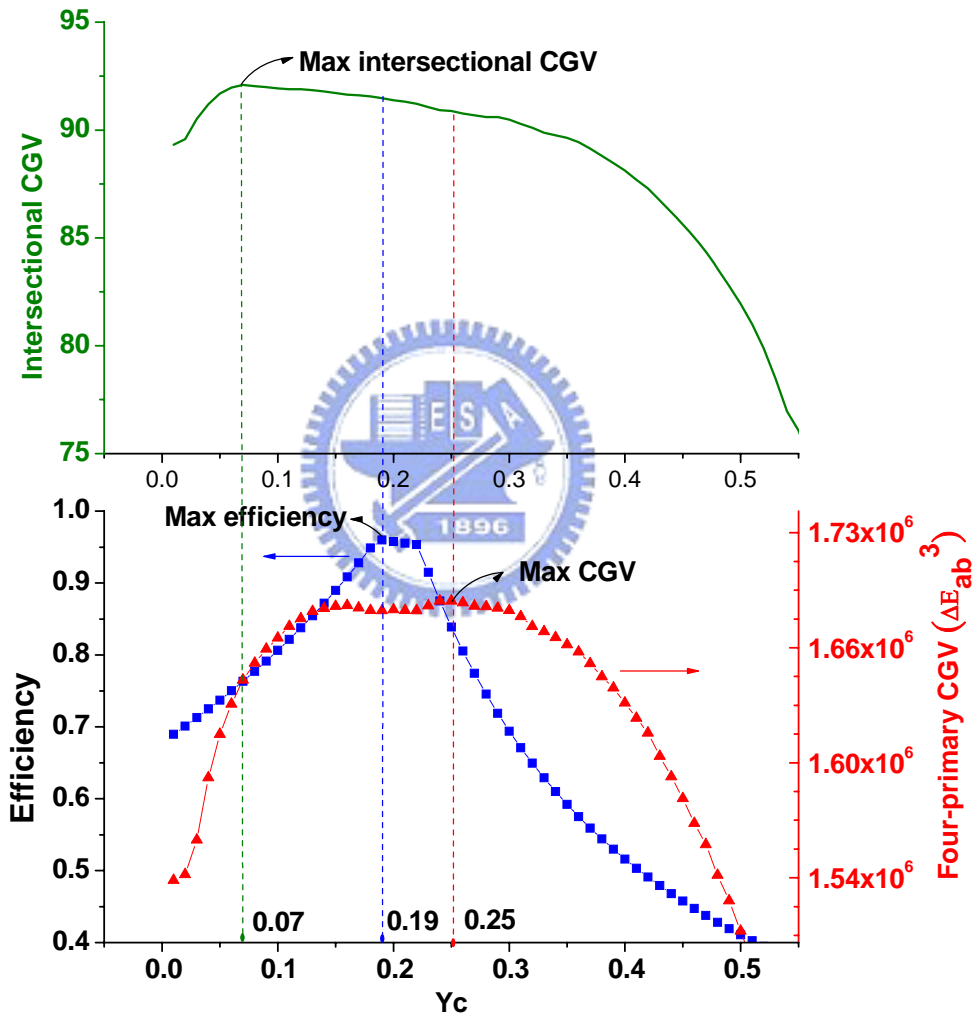


Fig. 4-18. Efficiency, four-primary CGV, and the intersectional CGV plotted against Y_c for comparison with real surface gamut input

As shown in Table 4-5, the comparisons of computed data are based on three criteria including the maximum efficiency, four-primary CGV, and intersectional CGV. The first row fulfills the maximum white point luminance requirement at $Y_c=0.19$, the maximum efficiency

is 0.96, the four-primary CGV is about 1.684×10^6 , and the intersectional CGV is about 91.5 % of real surface CGV. Besides, the second row fulfills the maximum CGV requirement at $Y_c=0.25$, the maximum efficiency is 0.84, the four-primary CGV is about 1.865×10^6 , and the intersectional CGV was about 90.9% of real surface CGV. Furthermore, the third row fulfills the maximum intersection CGV requirement at $Y_c=0.07$, the maximum efficiency is 0.76, the four-primary CGV is about 1.646×10^6 , and the intersectional CGV was about 92.1 % of real surface CGV. Obviously, each criterion has the largest value, which will be discussed in next section.

Table 4-5 The compared results of each criterion

TEST INPUT	Criteria Used	Y_c	η_{\max}	Four-primary CGV (ΔE_{ab}^3)	Intersectional CGV (with test input)
"Real Surface Color "	Max White Point Luminance	0.19	0.96	1.685×10^6	91.5% Input CGV
	Max CGV	0.25	0.84	1.690×10^6	90.9 % Input CGV
	The Proposed Design	0.07	0.76	1.646×10^6	92.1% Input CGV

With the three criteria setting, the LED backlight was set to achieve the white point illuminance C and measured the color difference. As shown in Table 4-6, the measured color difference in $\Delta u'v'$ is lower than the minimum perceptible limit. Consequently, the designed relative luminance is also acceptable.

Table 4-6 The color difference with the reference white C in CIE 1976 UCS diagram of each criterion

criteria	result	$\Delta u'v'$ (with D65)
Max White Point Luminance		7.297×10^{-4}
Max CGV		4.608×10^{-3}
The Proposed Design		4.724×10^{-3}

4.3 Discussion

Since the MPD offers the flexibility to design its CGV, the optimal design of display CGV may depend on the preference of its application. The comparison condensed from Table 4-2 and Table 4-5 is shown in Table 4-7, which divides the above results into four levels from high to low, i.e. excellent (⊙), good (○), fair (△), and poor (X). As shown in Table 4-7, there is an excellent outcome at each criterion. Each criterion of CGV design of MPD can be applied to specific applications to get the preferred results.

Table 4-7 The condensed comparison of each criterion

TEST INPUT	Criteria Used	Yc	η_{\max}	Four-primary CGV	Intersectional Input CGV
sRGB Color Space	Max White Point Luminance	0.20	⊙	△	△
	Max CGV Design	0.24	○	⊙	X
	The Proposed Design	0.04	△	△	⊙
"Real Surface Color "	Max White Point Luminance	0.19	⊙	○	△
	Max CGV Design	0.25	△	⊙	X
	The Proposed Design	0.07	X	△	○

⊙: Excellent ○: Good △: Fair X: Poor

The first and fourth rows in Table 4-7 are the results of maximum efficiency setting for sRGB color space and real surface color gamut inputs, respectively. Usually, the display of high luminance is preferred. From Table 4-7, this criterion sacrifices a little color reproducibility to have the great luminance output. It can meet the need of the display application which requires less performance in color perception but higher luminance.

The results of maximum CGV design are at the second and fifth rows. In general, the larger color gamut can represent more colors. There are some applications, such as computer

graph (CG) or electronic art, which are preferred the large gamut design. However, in order to represent the vivid color, there must have the corresponding input gamut. From Table 4-7, the largest CGV does not have the maximum input color intersection. Therefore, some colors from input signal cannot be reproduced on largest gamut display by this setting.

The third and sixth rows are the results of proposed design. The excellent input CGV intersection of the proposed design is much better than the other criteria. Therefore, the proposed criterion can cover the maximum original input color to achieve the more natural and fidelity color reproduction. However, the efficiency of the proposed design is not good enough. The choice of the available luminance of LEDs may have the chance to match the relative luminance ratio, thus achieving the highest efficiency. Alternatively, from the above plots, the proper Y_c may be a compromising result of the requirements of maximum CGV intersection and maximum white point luminance, depending on the preference of its application. Furthermore, when different input color gamut is chosen, the result may have maximum input color reproduction and maintain high efficiency simultaneously.

Nowadays, some new color encoding standards, such as “xvYcc” [30], etc., have been developed to fulfill the increasing demand of color performance of displays. From the comparison, it depicts that if using the proposed method to design a large gamut display may cover the largest CGV of such standard to achieve the best color performance and reproduce the most original input colors. Consequently, the proposed design can utilize of the input encoding gamut more properly and provide the best original color reproduction on MPDs.

Chapter 5

Conclusions & Future Work

5.1 Conclusions

The method for designing optimal four-primary color gamut has been presented and demonstrated in this thesis. Under the requirement of white point of input gamut and maximum available efficiency of LEDs, the initial four-primary CGV can be defined by setting the relative luminance of each primary. Furthermore, the maximum CGV intersection with input encoded CGV concept has been taken to ensure the maximum original color reproduction.

A four-primary LED backlight was constructed to enlarge the color gamut to about 147% of NTSC in CIE 1976 USC diagram for verifying these methods. The simulations of two input color gamuts, sRGB and real surface color, are demonstrated and compared with the experimental data. Two considered criteria proposed by Wen and our proposed one were examined in both input cases.

From the comparison of three criteria, it shows there is an excellent outcome at each criterion. The optimal design of display CGV may depend on the preference of its application. The maximum luminance requirement is most proper for the application which requires less performance in color perception, but higher luminance. The maximum CGV requirement can represent more colors and are suitable for large gamut demand. Different from the maximum CGV criterion, the proposed design attempts to reproduce the maximum original input colors which can achieve more natural and high-fidelity color reproduction.

Along with the explosive improvement of display technologies, the increasing demand of

color performance catches the manufacture's attention. The proposed method is suitable for the emerging demand on the application of MPDs. It is practical to apply to various input signals and reproduce the fidelity image on MPDs by the proposed method. Additionally, through the input encoding color gamut development and apply the optimal design on the proper MPD, the color reproduction perception has potential to increase toward the gamut range of human visual system.



5.2 Future work

So far, the optimum gamut design of maximum input color reproduction has been studied. For evaluating the gamut mapping of four-primary display, the further study will need to combine a fast-response LC module for displaying the input signal. Since the four-primary color gamut is larger than the other common input color gamut, the gamut mapping can be as similar color mapping or saturated color mapping. The flow chart of general gamut mapping is depicted in Fig. 5-1. The similar color mapping attempts to reproduce the original fidelity image, i.e. preserve the hue, lightness, and saturation, and the saturated color mapping attempt to reproduce the saturated color that people preferred, i.e. preserve hue and lightness, and enhance the saturation. Study will develop the gamut mapping algorithm for the two types of mapping and implement them to the FPGA board. Furthermore, in order to evaluate the preference color, there will need a psychological experiment. If so, both similar and preference color reproduction can be achieved on the four-primary display in the near future.

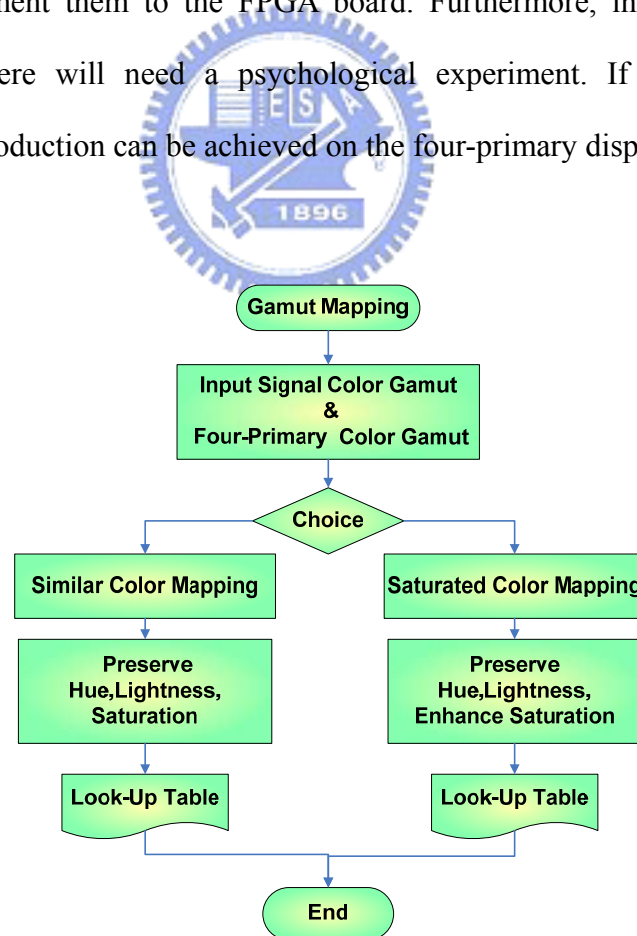


Fig. 5-1. The algorithm of two type gamut mappings of the large gamut display

Reference

- [1] J. A. C. Yule, *Principles of Color Reproduction*, Wiley, New York, 1967.
- [2] D den Engelsen, I Heynderickx, S Sluyterman, *Journal of the Society for Information Display*, 2004
- [3] JE Roddy, RJ Zolla, NA Blish, LS Horvath, US Patent 6,769,772, 2004
- [4] T. Ajito et al., Color conversion method for multi primary display using matrix switching, *Opt. Rev.* 8 (2001) 191–197.
- [5] <http://www.ntsc-tv.com/ntsc-index-01.htm>
- [6] J. A. Castellano, *Hanbook of display technology*, Chapter 8, Academic Press, Inc., San Diego (1992).
- [7] R. J. Johnson, “LED-based LCD backlight with extended color space,” US Patent, Patent No: US 6,608,614 B1.
- [8] Shmuel Roth, “Multi-primary liquid crystal display”, US Patent, Patent No: 2005/0,134,785 A1
- [9] G. Harber, M. Keuper, and S. Paolini, "Performance of high power LED illuminators in color sequential projection displays," 10th Int. Display Workshop, IDW'03, pp. 1585–1588 (2003)
- [10] Chino E, Jajiri K, Kawakami H, et al. Development of wide-color-gamut mobile displays with four-primary-color LCDs[J]. *SID'06 Digest*, 2006, 37(37): 1221-1224.
- [11] Y.K. Cheng et al., “Color Gamut Enlargement and Adjustment by Using Multi-color LEDs in Time Sequential”, IDMC 2005
- [12] Mark D. Fairchild, *Color Appearance Models*, 2nd Ed., Wiley-IS&T, Chichester, UK (2005).
- [13] R. W. G. Hunt: “The reproduction of COLOUR fifth edition”, Fountain Press, pp.222-242 (1995)
- [14] M. Yamaguchi, T. Teraji, K. Ohsawa, T. Uchiyama, H. Motomura, Y. Murakami, and N. Ohshima, "Color image reproduction based on the multispectral and multi-primary imaging: Experimental evaluation," *Proc. of SPIE*, vol. 4663, pp. 15-26, Jan. 2002.
- [15] H. Motomura, "Color conversion for a multi-primary display using linear interpolation on equi-luminance plane method (LIQUID)," *Journal of the SID*, vol. 11, no. 2, pp. 371-378, 2003
- [16] S.R. Fernandez and M.D. Fairchild, “Preferred Color Reproduction of Images with Unknown Colorimetry”, IS&T/SID 9th Color Imaging Conference, p.274 (2001).
- [17] Ján Morovic and M. Ronnier Luo., The fundamentals of gamut mapping: A survey. *Journal of Imaging Science and Technology*, 45(3), 283–290 (2001).

-
- [18] S. Wen, " Design of relative primary luminances for four-primary displays," *Displays*, 26, pp. 171-176 (2005).
- [19] Foley, J.D., van Dam, A., Feiner, S.K., Hughes, J.F. & Phillips, R.L., *Introduction to computer graphics*. 2nd rev. pr. Reading, Massachusetts, USA: Addison-Wesley, 1994. pp. 559 , ISBN 0-201-60921-5.
- [20] Hunt, R.W.G. *Measuring colour*. 2nd pr. Chichester, England : Ellis Horwood Limited, 1989. pp. 221, ISBN 0-7458-0125-0.
- [21] Hunt, R.W.G., *The reproduction of colour* 4th ed, Tolworth, England : Fountain Press, 1987.
- [22] Wright W.D, *Golden Jubilee of Colour in the CIE - The Historical and Experimental Background to the 1931 CIE System of Colorimetry*, Bradford. (1981).
- [23] W. R. J. brown and D.L. Macadam, *Visual sensitivities to combined chromaticity and luminance differences*, *J. Opt. Soc. Am.*, 39(10)808-834, 1949
- [24] S. Wen, " Design of relative primary luminances for four-primary displays," *Displays*, 26, pp. 171-176 (2005).
- [25] D. Travis, *Effective Color displays Theory and Practice*, Academic Press, London, 1991.
- [26] Gustav Braun, Kevin Spaulding, "Method for Evaluating the Color Gamut and Quantization Characteristics of Output-Referred Extended-Gamut Color Encodings", *Proc. Tenth Color Imaging Conference: Color Science and Engineering Systems*, p. 99-105, 2002;
- [27] sRGB color standard: <http://www.w3.org/Graphics/Color/sRGB>
- [28] Pointer M.R, "The gamut of real surface colours, *Colour Research and Application*, 1980
- [29] IEC 61966-2-1 : *Colour Measurement and Management in Multimedia Systems and Equipment - Part 2-1: Default RGB Colour Space – sRGB*, (1999).
- [30] Matsumoto et al, a new standard for video systems using extended-gamut ycc color space, *SID '06 Digest*, pp. 1130-1133.

Appendix – Measurement Data

	Digital Count	0	15	31	47	63	79	95	111	127
Color										
Cyan	X	6.78349	9.20351	17.7158	27.0343	35.3668	43.2582	50.903	57.9711	64.4909
	Y	6.11936	24.351	90.939	158.8	220.438	275.601	325.945	372.604	414.974
	Z	13.8776	20.8283	52.9623	92.4462	131.252	167.694	203.724	237.756	269.335
	x	0.2533	0.169236	0.109616	0.097148	0.091374	0.088907	0.087677	0.08674	0.086126
	y	0.228501	0.44777	0.562682	0.570647	0.569524	0.566435	0.56142	0.557514	0.554185
LXHL-ME1D Cyan										
Green	X	2.42737	9.84448	40.566	72.9285	102.085	128.441	152.999	176.074	198.184
	Y	2.15435	30.3737	156.366	296.137	429.449	551.573	667.057	773.419	876.508
	Z	5.36264	8.03684	22.4391	42.0961	61.9203	82.2934	101.375	121.707	141.003
	x	0.244095	0.204009	0.18492	0.177372	0.172018	0.16849	0.166045	0.164371	0.163021
	y	0.21664	0.629441	0.712792	0.720245	0.723643	0.723557	0.723936	0.722012	0.720993
LXHL-MM1D Green										
Blue	X	4.31294	5.81235	31.5976	83.6312	133.249	178.704	223.214	264.103	306.138
	Y	3.92835	5.11998	14.5709	33.8747	52.9323	70.6029	89.2311	105.512	122.915
	Z	9.06723	13.3196	166.914	474.651	767.026	1035.93	1299.17	1541.45	1787.21
	x	0.24918	0.239665	0.148288	0.141231	0.13979	0.139044	0.138503	0.138197	0.138133
	y	0.22696	0.211116	0.068381	0.057206	0.055531	0.054934	0.055368	0.055211	0.05546
LXHL-MB1D Blue										
Red	X	5.69463	6.55015	70.9736	217.453	381.349	546.32	713.117	877.115	1041.15
	Y	5.05848	5.28297	32.8909	95.5974	165.722	236.527	307.983	378.547	448.644
	Z	11.5925	11.9314	12.1114	12.2729	13.1856	13.0249	13.3618	14.0431	14.2899
	x	0.254843	0.275627	0.611969	0.668421	0.680668	0.686442	0.68936	0.690802	0.692215
	y	0.226375	0.222305	0.283601	0.293854	0.295797	0.297192	0.297723	0.298138	0.298284

	Digital Count	143	159	175	191	207	223	239	255	
Color										
Cyan	X	70.7466	76.5723	82.735	88.974	94.6467	100.066	105.91	111.219	
	Y	453.048	489.299	523.223	558.39	589.098	618.388	648.463	675.689	
	Z	299.212	327.15	353.443	380.481	405.138	428.899	451.986	472.457	
	x	0.085961	0.085745	0.086236	0.086564	0.086921	0.087215	0.087793	0.088314	
	y	0.550479	0.547914	0.545364	0.543263	0.541011	0.538969	0.537537	0.536532	
LXHL-ME1D Cyan										
Green	X	217.448	237.134	255.477	273.264	290.598	306.732	322.355	337.296	
	Y	965.259	1053.58	1136.69	1216.4	1291.47	1361.07	1426.89	1487.89	
	Z	158.224	176.681	193.933	210.581	227.727	242.533	256.174	269.391	
	x	0.162162	0.161602	0.161072	0.16072	0.16057	0.160565	0.160742	0.161033	
	y	0.719842	0.717993	0.716657	0.715426	0.7136	0.712477	0.711517	0.710353	
LXHL-MM1D Green										
Blue	X	344.966	384.442	420.212	457.748	489.194	522.882	553.865	586.014	
	Y	138.985	155.358	170.392	186.281	200.109	214.905	228.567	243.654	
	Z	2017.07	2248.41	2462.96	2682.45	2870.57	3070.27	3254.54	3446.12	
	x	0.13793	0.137881	0.137614	0.137607	0.137419	0.137309	0.137198	0.137054	
	y	0.055571	0.05572	0.055801	0.055999	0.056212	0.056434	0.056618	0.056985	
LXHL-MB1D Blue										
Red	X	1213.28	1376.69	1536.72	1697.49	1851.13	2012.61	2131.71	2199.72	
	Y	522.742	593.255	662.014	731.551	797.732	867.223	919.046	949.5	
	Z	14.3832	14.6837	15.7556	15.441	16.6287	16.431	16.6981	17.5998	
	x	0.693142	0.693676	0.693939	0.694417	0.69448	0.694899	0.694944	0.694615	
	y	0.298641	0.298925	0.298947	0.299266	0.299281	0.299428	0.299612	0.299828	

Appendix – Simulated Data

Yc, Yr, Yg, Yb : relative luminance of cyan, red, green, blue primaries

η max : maximum efficiency

v_four : color gamut volume of four primaries

v_intersec. : intersectional color gamut volume (CGV) with input gamut

% intersec. : percentage of intersectional input CGV

sRGB color gamut as the input:

Yc	Yr	Yg	Yb	η max	v_four	v_intersec.	% intersec.
0.01	0.28	0.65	0.07	0.69	1.549E+06	7.712E+05	98.64
0.02	0.28	0.64	0.07	0.70	1.562E+06	7.716E+05	98.70
0.03	0.28	0.63	0.07	0.71	1.600E+06	7.728E+05	98.84
0.04	0.28	0.62	0.07	0.72	1.626E+06	7.730E+05	98.86
0.05	0.28	0.61	0.07	0.73	1.643E+06	7.727E+05	98.83
0.06	0.28	0.59	0.07	0.75	1.657E+06	7.725E+05	98.80
0.07	0.28	0.58	0.07	0.76	1.669E+06	7.712E+05	98.64
0.08	0.28	0.57	0.07	0.77	1.676E+06	7.694E+05	98.40
0.09	0.28	0.56	0.06	0.79	1.681E+06	7.679E+05	98.21
0.10	0.28	0.55	0.06	0.80	1.686E+06	7.662E+05	98.00
0.11	0.28	0.54	0.06	0.82	1.690E+06	7.646E+05	97.79
0.12	0.28	0.53	0.06	0.83	1.694E+06	7.633E+05	97.62
0.13	0.28	0.52	0.06	0.85	1.697E+06	7.622E+05	97.49
0.14	0.28	0.51	0.06	0.87	1.699E+06	7.608E+05	97.31
0.15	0.29	0.50	0.06	0.88	1.700E+06	7.598E+05	97.18
0.16	0.29	0.49	0.06	0.90	1.701E+06	7.583E+05	96.98
0.17	0.29	0.48	0.06	0.92	1.701E+06	7.566E+05	96.77
0.18	0.29	0.47	0.06	0.94	1.700E+06	7.549E+05	96.56
0.19	0.29	0.46	0.06	0.96	1.698E+06	7.527E+05	96.28
0.20	0.29	0.45	0.06	0.98	1.697E+06	7.510E+05	96.06
0.21	0.29	0.44	0.06	0.96	1.698E+06	7.501E+05	95.94
0.22	0.29	0.43	0.06	0.91	1.701E+06	7.500E+05	95.93
0.23	0.29	0.42	0.06	0.88	1.702E+06	7.488E+05	95.77
0.24	0.29	0.41	0.06	0.84	1.702E+06	7.474E+05	95.60
0.25	0.29	0.40	0.06	0.81	1.700E+06	7.450E+05	95.28
0.26	0.29	0.39	0.06	0.77	1.699E+06	7.430E+05	95.03
0.27	0.29	0.38	0.06	0.75	1.699E+06	7.407E+05	94.73

Yc	Yr	Yg	Yb	η max	v_four	v_intersec.	% intersec.
0.28	0.29	0.37	0.06	0.72	1.698E+06	7.380E+05	94.39
0.29	0.29	0.36	0.06	0.69	1.695E+06	7.352E+05	94.03
0.30	0.30	0.35	0.06	0.67	1.691E+06	7.320E+05	93.62
0.31	0.30	0.34	0.06	0.65	1.688E+06	7.289E+05	93.23
0.32	0.30	0.33	0.06	0.63	1.684E+06	7.257E+05	92.81
0.33	0.30	0.32	0.06	0.61	1.681E+06	7.222E+05	92.37
0.34	0.30	0.31	0.06	0.59	1.677E+06	7.191E+05	91.97
0.35	0.30	0.30	0.06	0.58	1.672E+06	7.148E+05	91.43
0.36	0.30	0.29	0.06	0.56	1.666E+06	7.106E+05	90.89
0.37	0.30	0.28	0.05	0.54	1.660E+06	7.067E+05	90.39
0.38	0.30	0.26	0.05	0.53	1.652E+06	7.018E+05	89.76
0.39	0.30	0.25	0.05	0.52	1.644E+06	6.969E+05	89.13
0.40	0.30	0.24	0.05	0.50	1.635E+06	6.918E+05	88.48
0.41	0.30	0.23	0.05	0.49	1.628E+06	6.866E+05	87.81
0.42	0.30	0.22	0.05	0.48	1.616E+06	6.806E+05	87.05
0.43	0.30	0.21	0.05	0.47	1.605E+06	6.737E+05	86.17
0.44	0.30	0.20	0.05	0.46	1.594E+06	6.660E+05	85.19
0.45	0.31	0.19	0.05	0.45	1.581E+06	6.592E+05	84.32
0.46	0.31	0.18	0.05	0.44	1.566E+06	6.506E+05	83.22
0.47	0.31	0.17	0.05	0.43	1.553E+06	6.414E+05	82.04
0.48	0.31	0.16	0.05	0.42	1.538E+06	6.327E+05	80.92
0.49	0.31	0.15	0.05	0.41	1.518E+06	6.214E+05	79.48
0.50	0.31	0.14	0.05	0.40	1.499E+06	6.105E+05	78.08
0.51	0.31	0.13	0.05	0.39	1.479E+06	5.979E+05	76.47
0.52	0.31	0.12	0.05	0.39	1.457E+06	5.860E+05	74.95
0.53	0.31	0.11	0.05	0.38	1.439E+06	5.730E+05	73.28
0.54	0.31	0.10	0.05	0.37	1.409E+06	5.554E+05	71.03
0.55	0.31	0.09	0.05	0.37	1.379E+06	5.405E+05	69.14
0.56	0.31	0.08	0.05	0.36	1.356E+06	5.308E+05	67.88
0.57	0.31	0.07	0.05	0.35	1.338E+06	5.183E+05	66.29
0.58	0.31	0.06	0.05	0.35	1.330E+06	5.115E+05	65.43
0.59	0.31	0.05	0.05	0.34	1.321E+06	5.031E+05	64.35
0.60	0.32	0.04	0.05	0.34	1.308E+06	4.914E+05	62.85
0.61	0.32	0.03	0.05	0.33	1.296E+06	4.851E+05	62.04
0.62	0.32	0.02	0.05	0.32	1.282E+06	4.781E+05	61.16

Real surface color gamut as the input

Yc	Yr	Yg	Yb	η max	v_four	v_intersec.	% intersec.
0.01	0.28	0.63	0.07	0.69	1.535E+06	7.658E+05	89.32
0.02	0.28	0.62	0.07	0.70	1.538E+06	7.681E+05	89.58
0.03	0.28	0.61	0.07	0.71	1.557E+06	7.760E+05	90.51
0.04	0.29	0.60	0.07	0.72	1.592E+06	7.819E+05	91.19
0.05	0.29	0.59	0.07	0.74	1.616E+06	7.861E+05	91.69
0.06	0.29	0.58	0.07	0.75	1.633E+06	7.885E+05	91.97
0.07	0.29	0.57	0.07	0.76	1.646E+06	7.896E+05	92.09
0.08	0.29	0.56	0.07	0.78	1.655E+06	7.891E+05	92.03
0.09	0.29	0.55	0.07	0.79	1.663E+06	7.887E+05	91.99
0.10	0.29	0.54	0.07	0.81	1.669E+06	7.882E+05	91.93
0.11	0.29	0.53	0.07	0.82	1.676E+06	7.879E+05	91.90
0.12	0.29	0.52	0.07	0.84	1.680E+06	7.878E+05	91.89
0.13	0.29	0.51	0.07	0.85	1.684E+06	7.875E+05	91.84
0.14	0.29	0.50	0.07	0.87	1.686E+06	7.869E+05	91.78
0.15	0.29	0.49	0.07	0.89	1.687E+06	7.864E+05	91.71
0.16	0.29	0.48	0.07	0.91	1.687E+06	7.858E+05	91.64
0.17	0.29	0.47	0.07	0.93	1.686E+06	7.854E+05	91.60
0.18	0.29	0.46	0.07	0.95	1.685E+06	7.850E+05	91.56
0.19	0.30	0.45	0.07	0.96	1.685E+06	7.843E+05	91.48
0.20	0.30	0.44	0.07	0.96	1.685E+06	7.835E+05	91.38
0.21	0.30	0.43	0.07	0.96	1.685E+06	7.829E+05	91.31
0.22	0.30	0.42	0.07	0.95	1.685E+06	7.820E+05	91.21
0.23	0.30	0.41	0.07	0.91	1.687E+06	7.808E+05	91.06
0.24	0.30	0.40	0.07	0.88	1.690E+06	7.795E+05	90.92
0.25	0.30	0.38	0.07	0.84	1.690E+06	7.792E+05	90.88
0.26	0.30	0.37	0.07	0.81	1.689E+06	7.782E+05	90.76
0.27	0.30	0.36	0.07	0.77	1.687E+06	7.775E+05	90.68
0.28	0.30	0.35	0.06	0.75	1.687E+06	7.768E+05	90.60
0.29	0.30	0.34	0.06	0.72	1.686E+06	7.768E+05	90.60
0.30	0.30	0.33	0.06	0.69	1.685E+06	7.757E+05	90.47
0.31	0.30	0.32	0.06	0.67	1.681E+06	7.741E+05	90.28
0.32	0.30	0.31	0.06	0.65	1.676E+06	7.725E+05	90.10
0.33	0.30	0.30	0.06	0.63	1.673E+06	7.706E+05	89.88
0.34	0.31	0.29	0.06	0.61	1.670E+06	7.695E+05	89.75
0.35	0.31	0.28	0.06	0.59	1.666E+06	7.685E+05	89.64

Yc	Yr	Yg	Yb	η max	v_four	v_intersec.	% intersec.
0.36	0.31	0.27	0.06	0.58	1.662E+06	7.668E+05	89.43
0.37	0.31	0.26	0.06	0.56	1.655E+06	7.642E+05	89.13
0.38	0.31	0.25	0.06	0.54	1.648E+06	7.614E+05	88.80
0.39	0.31	0.24	0.06	0.53	1.642E+06	7.585E+05	88.46
0.40	0.31	0.23	0.06	0.52	1.633E+06	7.556E+05	88.12
0.41	0.31	0.22	0.06	0.50	1.625E+06	7.519E+05	87.69
0.42	0.31	0.21	0.06	0.49	1.617E+06	7.484E+05	87.29
0.43	0.31	0.20	0.06	0.48	1.604E+06	7.436E+05	86.73
0.44	0.31	0.19	0.06	0.47	1.592E+06	7.390E+05	86.20
0.45	0.31	0.18	0.06	0.46	1.580E+06	7.340E+05	85.61
0.46	0.31	0.17	0.06	0.45	1.566E+06	7.290E+05	85.03
0.47	0.31	0.16	0.06	0.44	1.555E+06	7.233E+05	84.36
0.48	0.31	0.15	0.06	0.43	1.537E+06	7.165E+05	83.57
0.49	0.32	0.14	0.06	0.42	1.523E+06	7.096E+05	82.77
0.50	0.32	0.13	0.06	0.41	1.506E+06	7.025E+05	81.94
0.51	0.32	0.12	0.06	0.40	1.488E+06	6.945E+05	81.00
0.52	0.32	0.11	0.06	0.39	1.467E+06	6.848E+05	79.87
0.53	0.32	0.10	0.06	0.39	1.444E+06	6.729E+05	78.48
0.54	0.32	0.09	0.06	0.38	1.417E+06	6.599E+05	76.96
0.55	0.32	0.08	0.05	0.37	1.399E+06	6.522E+05	76.07
0.56	0.32	0.07	0.05	0.37	1.367E+06	6.398E+05	74.62
0.57	0.32	0.05	0.05	0.36	1.360E+06	6.339E+05	73.94
0.58	0.32	0.04	0.05	0.35	1.355E+06	6.301E+05	73.49
0.59	0.32	0.03	0.05	0.35	1.345E+06	6.220E+05	72.55
0.60	0.32	0.02	0.05	0.34	1.336E+06	6.167E+05	71.93
0.61	0.32	0.01	0.05	0.34	1.324E+06	6.073E+05	70.83
0.62	0.32	0.00	0.05	0.33	1.314E+06	6.013E+05	70.13